UNIVERSITÄTSKLINIKUM HAMBURG-EPPENDORF

III. Medizinische Klinik und Poliklinik Nephrologie,

Rheumatologie und Endokrinologie

Prof. Dr. med. Tobias B. Huber

Treatment of Type 2 diabetic nephropathy mice with the sodium-glucose cotransporter-2 inhibitor (SGLT2i) and/or angiotensin receptor blocker (ARB)

Dissertation

zur Erlangung des Grades eines Doktors der Medizin
an der Medizinischen Fakultät der Universität Hamburg.

vorgelegt von:

Zhouning Liao

aus (Hunan) China

Hamburg 2024

Contents

1. Introduction

1.1 Diabetic nephropathy

Diabetes mellitus (DM) is a complex metabolic disease caused by a combination of genetic and environmental factors[1]. Diabetic nephropathy (DN) is one of the most common diabetes complications, a common microvascular complication of chronic hyperglycemia which can lead to different types of renal cell dysfunction and even renal failure. The global incidence of DN has doubled in the past 10 years to become the major cause of end-stage renal disease (ESRD).

In 2019, the global prevalence for diabetes were 537 million people, according to the data from the International Diabetes Federation. By 2030, 643 million people are expected to have diabetes, with type 2 diabetes accounting for approximately 85-90% of all cases[2]. Globally, the prevalence of diabetes is increasing year on year, with higher growth rates, especially in developing countries[3].

Currently, the main therapeutic aim is to prevent the onset and to delay the progression of DN by controlling the patient's blood glucose and blood pressure with medication. However, there is still much to learn about the intricate pathogenesis of DN, the risk of poor treatment outcomes and disease progression remain. It is therefore important to understand the pathogenic mechanisms of DN and to find new therapeutic agents and approaches to improve the prognosis of DN[4]. Several pathways and factors have been found to play an essential role in the development and progression of DN, such as hemodynamic and metabolic changes, inflammation, oxidative stress, and the

renin-angiotensin system[5].

1.2 The pathogenesis of DN

Characteristic pathological changes in the glomerulus include increased mesangial matrix, proliferation, and hypertrophy of mesangial cells, thickening of the glomerular basement membrane (GBM), and Kimmelstiel-Wilson nodules (Figure 1)[6, 7]. Characteristic changes in the tubular interstitium include tubular hypertrophy, interstitial fibrosis, and thickening of the tubular basement membrane (TBM) (Figure 1d).

Diffuse mesangial expansion is one of the prominent signs of diabetic glomerulopathy. Mesangial matrix expansion may aggravate proteinuria and renal impairment. Increased matrix in the mesangial area reduces the area of capillaries available for filtration, leading to further loss of renal function[8, 9].

The other distinctive feature of diabetic glomerulopathy is GBM thickening[10]. The thickened GBM results in an increased permeability to proteins, which is one of the causes of proteinuria[11]. On the other hand, increased permeability of the GBM results from the reduction of negatively charged proteoglycans, leading to the passage of positively charged proteins, and this dysregulation of charge selectivity contributes to the development of proteinuria[11, 12].

The glomerular endothelium is characterized by a hydrated meshwork of proteoglycans that make up the first component of the glomerular filtration barrier (GFB). Studies have shown that the glomerular endothelial surface layer restricts the passage of macromolecules, preventing plasma albumin from being filtered by the glomerulus. In addition, the glomerular endothelium may

2

influence albumin filtration by increasing contact between podocytes and plasma components[13].

The slit diaphragm of podocytes forms the third layer of the renal filtration barrier. During the progression of kidney disease, the podocytes change by decreasing in number and effacement of foot processes[14]. In conclusion, the GFB, consisting of glomerular endothelium, podocytes, and GBM, collectively influences glomerular filtration rate and proteinuria development.
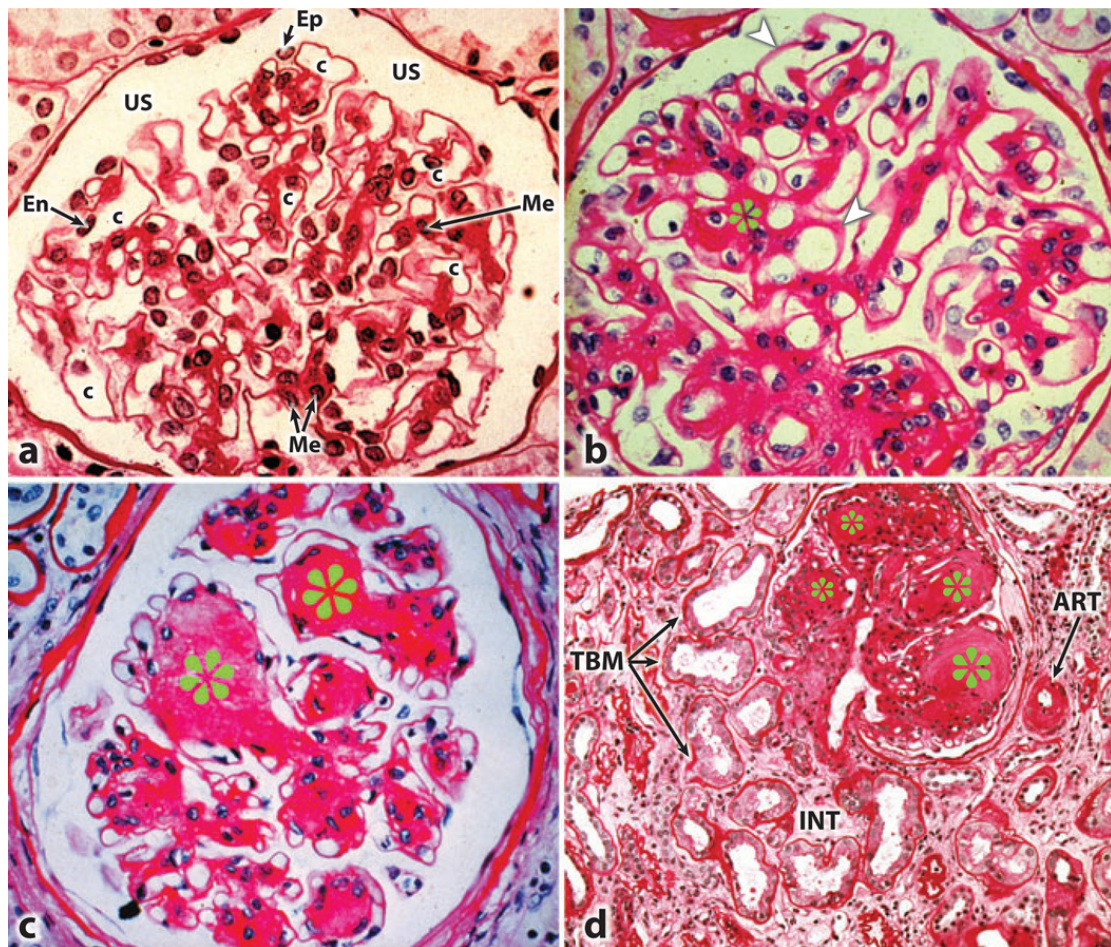
Figure 1. Light micrographs showing different stages of development of glomerulopathy and tubulointerstitial disease in diabetic nephropathy. (a) A normal glomerulus. (b) Expanded mesangial regions (asterisks) and thickened basement membranes (arrowheads). (c) Mesangial regions were characteristic of Kimmelstiel-Wilson nodular (asterisks). (d) Tubular basement membrane (TBM), fibrosis of the interstitium (INT), and hyalinization of afferent arteriole (ART). Abbreviations: En, endothelial cell; c, capillary lumen; Me, mesangium; Ep, visceral epithelial cell (podocyte); US, urinary space (Yashpal S. Kanwar，2011).

1.3 The diagnosis of DN

DN is a clinical syndrome in patients with DM defined by persistent albuminuria (>200µg/min/day or >300mg/day) at 2 or more of 3 examinations within 6 months, and a gradual decrease in glomerular filtration rate (GFR) (<60 ml/min^{-1}/1.73 m^2) [15].

Typically, the clinical presentation of DN is the development of proteinuria accompanied by a decreased renal function. However, some patients with diabetes develop vascular complications and decreased renal function in the absence of proteinuria, which is known as nonproteinuric DN (NP-DN)[16]. Some recent data demonstrate that estimated glomerular filtration rate (eGFR) is decreased in DN without albuminuria[17, 18].

In contrast to the traditional perspective that albuminuria typically precedes and leads to a gradual decline in GFR, this viewpoint suggests that the initiation and progression of deteriorating renal function may not necessarily be associated with albuminuria. eGFR and albuminuria can manifest simultaneously and advance either concurrently or independently[19]. Consequently, there are two distinct pathways contributing to the development and advancement of DN: albuminuria and non-albuminuria. The prevalence of NP-DN is estimated to be 50-60% in type 1 DM and 45-70% in type 2 DM[20].

1.4 Molecular mechanisms of DN

1.4.1 Role of hyperglycemia

Hyperglycemia is the most important factor contributing to the development of DN (Figure 2).The uptake of glucose into kidney cells is influenced by various

facilitated transporters like the glucose transporter-1 (GLUT-1) and glucose transporter-4 (GLUT-4), along with energy-dependent transporters like sodium-glucose-linked transporters 1 and 2 (SGLT1 and SGLT2)[21].
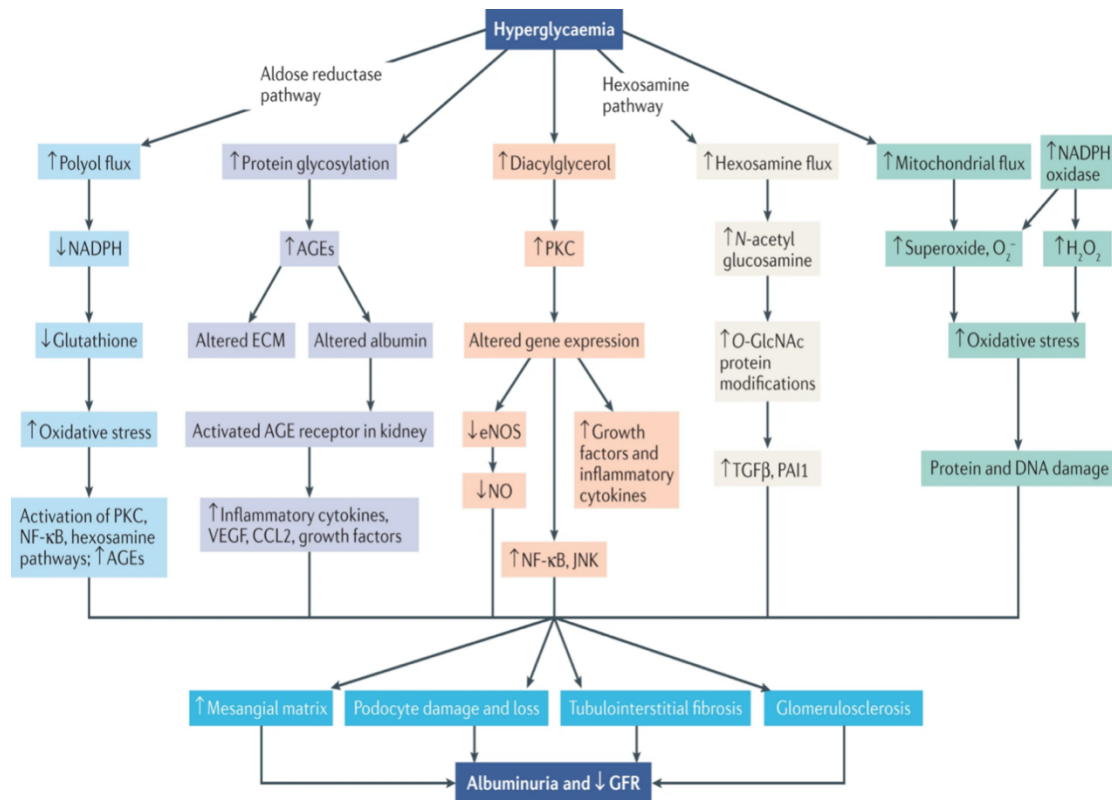
Figure 2. **Effects of hyperglycemia.** Effects of hyperglycemia on multiple biochemical pathways and cells in DN (Ralph A. DeFranzo，2017).

It has been shown that GLUT-1 and GLUT-4 are saturated at normal glucose concentrations. When glucose concentrations increase, increased expression or activity of GLUT-1 and GLUT-4 are required to increase glucose metabolic flux. Overexpression of GLUT-1 in mice results in an increased expression of extracellular matrix (ECM) proteins, including fibronectin and type IV collagen and thus mimics a DN phenotype[22]. Based on these studies it was speculated that increased GLUT-1 expression may play an important role in the pathobiology of diabetic complications[22]. Furthermore, down-regulation of GLUT-1 reduced the expression of fibronectin in glucose-induced mesangial cells, suggesting that glucose transport in early steps can significantly influence

downstream cellular events and ultimately distal processes such as ECM synthesis[21].

ECM structural proteins irreversibly cross-link with glucose to produce extracellular advanced glycation end products (AGEs). Moreover, extracellular AGEs can regulate cellular function by interacting with their cognate receptors for AGEs (RAGE) or binding proteins, including galectin-3, OST-48 (AGE-R1) , macrophage scavenger receptor 2 (MSR2), and 80K-H (AGE-R2), which may alter matrix and cellular function[7, 23].

Furthermore, Protein kinase C (PKC) activation and associated cell signaling are induced by excess glucose. In signaling kinases, PKC appears to be central to the mechanism of DN[24]. In addition, high glucose upregulates transforming growth factor β1 (TGF-β1) and ECM genes and activates transcription factors including nuclear factor-κB (NK-κB), specificity protein 1 (Sp1) and activator protein-1 (AP-1)[25]. Consequently, PKC inhibitors can mitigate hyperglycemia or ECM accumulation and TGF-β1 production in renal glomeruli or mesangial cells[26]. Moreover, significantly reduced expression of NADPH oxidase subunit, NOX 2 and 4 activations in DM provide additional evidence supporting the role of PKC activation in regulating overproduction of oxidants, ECM, and fibrotic factors in renal glomeruli[27].

1.4.2 Hemodynamic changes

Systemic hypertension plays an important role in the progression of DN. In addition, intrarenal hemodynamic abnormalities caused by inflammation, vascular remodeling, and matrix accumulation lead to a decrease in glomerular arteriolar resistance and leakage of albumin from the glomerular capillaries.

This results in the early manifestation of DN with glomerular hyperfiltration and microalbuminuria[28]. It was shown that increased intra-glomerular pressure due to vasodilation of the afferent arteriole in comparison to the efferent arteriole led to increased mechanical stress on the vessels, which led to increased expression of GLUT-1, further activating increased glucose uptake and finally the production of AGEs, polyphenols, and PKC[29].

Another hypothesis is that abnormal tubular sodium reabsorption is linked to glomerular hyperfiltration[30]. Tubuloglomerular feedback is a physiological process that self-regulates glomerular blood flow (Figure 3). Tubuloglomerular feedback occurs when a rise in sodium chloride reabsorption in the proximal renal tubule causes an increase in GFR due to a macular-glomerular pathway[31]. When GFR is increased, delivery of sodium chloride to the macular densa cells in juxtaglomerular apparatus (JGA) is increased. The result is that luminal Na-2Cl-K cotransporter activation in the loop of Henle transports sodium chloride from the luminal fluid to the surrounding interstitium. Consequently, adenosine release is increased, leading to an increase in cytosolic calcium via A_1 receptors in extraglomerular mesangial cells[32]. This signal is transmitted to smooth muscle cells in afferent arterioles, regulating afferent arteriolar vasoconstriction, which results in a decrease in GFR[33].
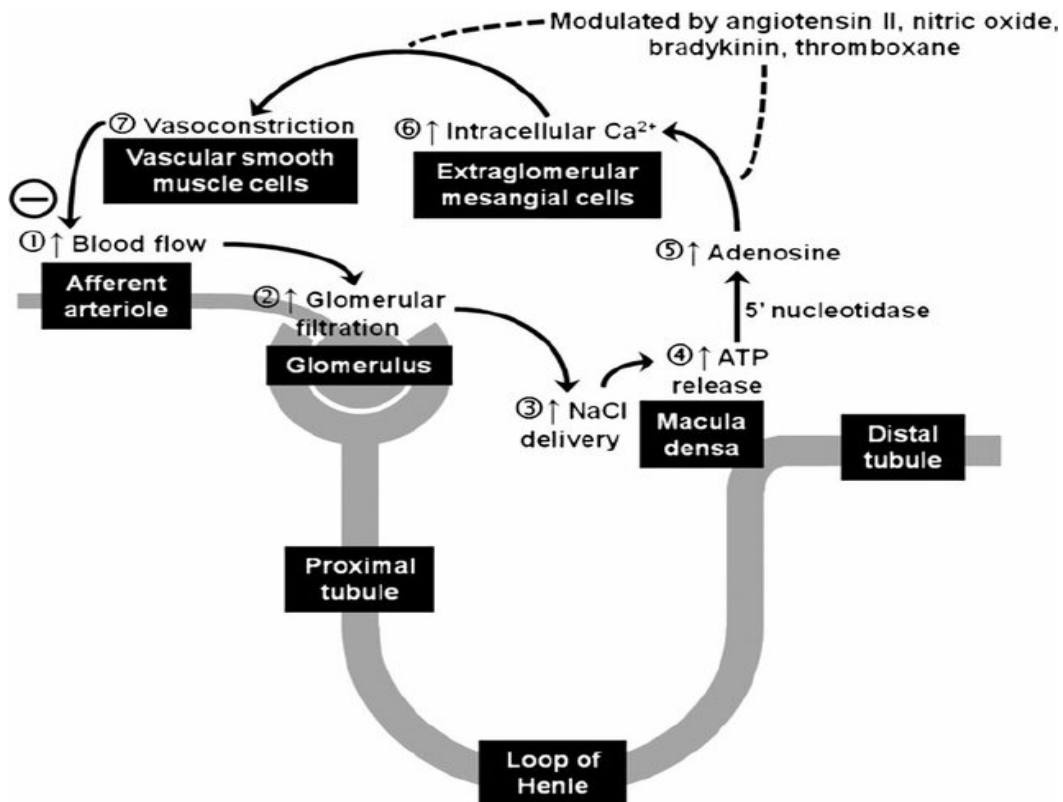
Figure 3. **The function of tubuloglomerular feedback** (Anil Chalisey, 2012).

1.4.3 The Renin-Angiotensin-Aldosterone System (RAAS)

RAAS plays a key role in the progression of DN, and hypertension which usually accompanies DM. The progression of DN is accelerated when progressing from normoalbuminuric to macroalbuminuria, and the risk of cardiovascular and renal disease deepens with increased albumin excretion[34, 35]. It has been shown that inhibition of RAAS reduces urinary protein, and in patients with DN, reduced urinary albumin excretion significantly reduces the risk of progression to stroke, myocardial infarction, and ESRD[36].
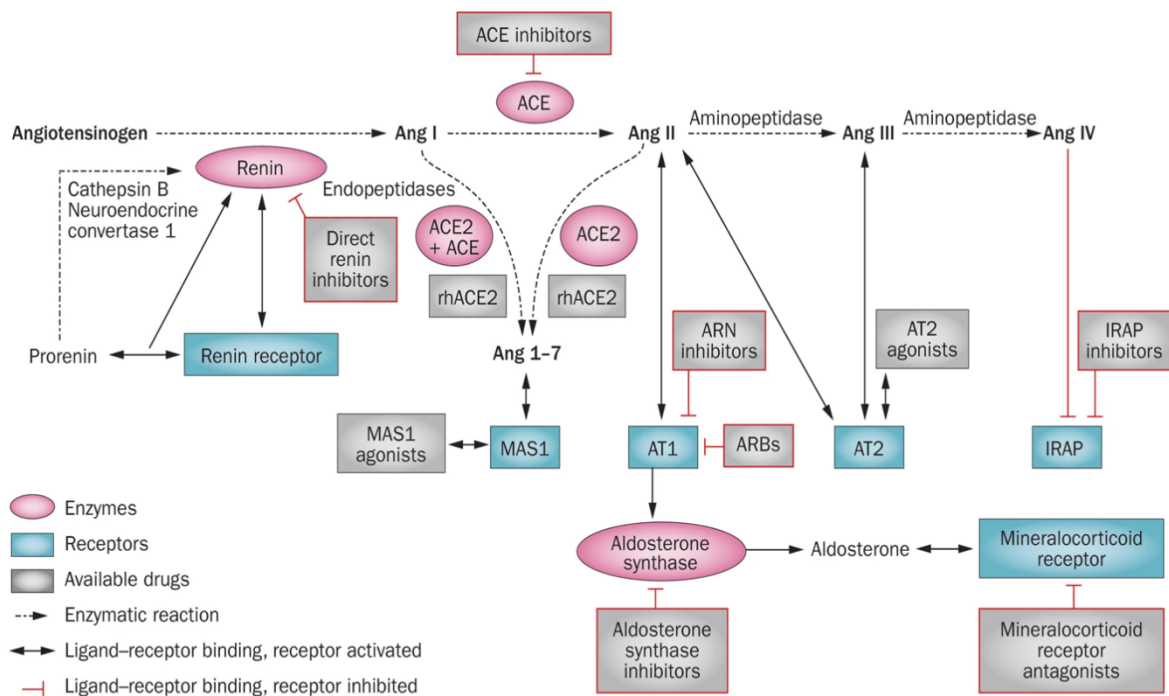
Figure 4. Signaling pathways of the RAAS cascade. Abbreviations: ARN, angiotensin receptor–neprilysin; AT2, type-2 Ang II receptor; IRAP, leucyl-cystinyl aminopeptidase; rh, recombinant human; MAS1, proto-oncogene Mas (Cesar A. Romero, 2015).

When blood volume is reduced, juxtaglomerular cells begin to secrete renin, which is the beginning of the RAAS cascade (Figure 4). Renin is a rate-limiting step in the generation of Angiotensin II (Ang II). Renin changes angiotensinogen to Ang I, which proceeds to three key pathways including ACE-Ang II-AT1-aldosterone, Ang IV-IRAP and ACE2-Ang 1-7-MAS1.

Angiotensin I (Ang I) stimulate the secretion of adrenaline and norepinephrine. Ang I can be transformed into Ang II by endothelial angiotensin-converting enzyme (ACE). Increased Ang II causes vasoconstriction and elevated blood pressure and is the most prominent mediator of RAAS. In multiple tissues, including the adrenal grand and vascular smooth muscle, Ang II connects to the type-1 Ang II receptor (AT1) and raises blood pressure. When aldosterone combines with the mineralocorticoid receptor, AT1 receptors in the adrenal

gland stimulate aldosterone secretion, leading to sodium and water retention[37].

Angiotensin-converting enzyme inhibitors (ACEi) reduce Ang II production, which can lead to a reduction in intraglomerular pressure and glomerular hypertension. They also reduce the permeability of urinary albumin in the glomerulus, thereby reducing proteinuria[38]. On the other hand, Angiotensin II receptor blockers (ARBs) block AT1 and antagonize Ang II, leading to lower blood pressure and alleviation of interstitial fibrosis[39, 40].

Ang II has a variety of biochemical and physiological effects that contribute to the development of DN (Table 1). Ang II directly increases matrix accumulation and cytokine formation[41], increases proteinuria, and accelerates tubulointerstitial damage[42]. Recent studies have shown that Ang II increases superoxide production in mesangial cells, which may contribute to oxidative-induced renal injury. On the other hand, Ang II acts directly on circulation by constricting blood vessels, regulating aldosterone secretion, and enhancing myocardial contractility and heart rate during systemic blood deficit[43]. The role of Ang-II goes beyond its classical role as a hemodynamic mediator.

Furthermore, oxidative stress, fibrosis, and inflammation are major links in the pathogenesis and progression of DN. Oxidative stress activates pathological pathways in the kidney in all cell types, including endothelial cells, epithelial cells, mesangial cells, and podocytes, and is a very important part of DN[44]. Overall, oxidative stress is a component of cellular injury and Ang-II is a major molecule that plays a core role in kidney injury. Despite this, studies on oxidative stress and Ang-II as a therapeutic approach have yielded inconclusive results[45, 46].

Table 1. Proposed mechanisms of angiotensin II effects in diabetic nephropathy (DAVID J. LEEHEY, 2000).

Hemodynamic effects	Non-hemodynamic effects
Systemic hypertension	Induction of renal hypertrophy and cell proliferation
Systemic and renal vasoconstriction	Stimulation of extracellular matrix synthesis
Increased glomerular capillary pressure and permeability	Inhibition of extracellular matrix degradation
Mesangial cell contraction leads to a reduction in filtration surface area	Stimulation of cytokine (e.g., TGF-β, VEGF, endothelin) production
	Stimulation of superoxide production

1.4.4 Oxidative stress

Oxidative stress is involved in multiple pathways in the pathogenesis of DN, including an increase in reactive oxygen species (ROS) due to hyperglycemia, which is central to the pathogenesis of DN[16].

In diabetes, ROS-causing factors include AGE, NADPH oxidase (NOX), and polyol chains. ROS can be generated via the mitochondrial respiratory chain, uncoupled nitric oxide synthase (NOS), NOX, xanthine oxidative (XO), and lipoxygenase (LOX)[47]. Hyperglycemia-induced oxidative stress is caused by increased levels of proinflammatory proteins, and cytokines secreted by macrophages cause an inflammatory response[48]. Oxidative stress can cause injury to endothelial cells, podocyte, and interstitial cells, leading to proteinuria and tubular fibrosis[49, 50]. In addition, oxidative stress can interact with other pathogenic pathways to exacerbate the damage to DN[51]. On the one hand,

Chronic hyperglycemia-induced oxidative stress activates PKC, increases TGF-β, and Ang-II expression, which are pro-oxidative stress stimulators[52]. On the other hand, Ang-II and TGF-β produced by oxidative stress further increase the ROS response by activating NOX. As a result of the increase in TGF-β produced by continuously activated ROS leads to extracellular matrix remodeling, thereby exacerbating the process of tubulointerstitial fibrosis in the kidney.

1.5 The treatment of DN

It has been shown that the treatment of DN is primarily based on strict control of the patient's blood pressure and blood glucose. Despite this, it can only delay the progression of DN and cannot stop or reverse its development. Consequently, targeting the different pathological mechanisms of DN has become a focus for the development of new therapies[53].

1.5.1 Blood pressure and albuminuria control

The incidence of hypertension has increased in patients with DN, and controlling blood pressure is a very important factor in the treatment of DN. Regardless of the type of antihypertensive drug, good control of blood pressure will have a positive impact on the progression of albuminuria and diabetic nephropathy. Drugs that inhibit the RAAS, including ARBs and ACEi , lower urinary protein in addition to blood pressure and have a protective effect on the kidneys[54]. Additionally, in patients with T2DM, ARBs play a significant role in delaying the progression from microalbuminuria to microalbuminuria. In an over 2-year follow-up study, 590 patients with T2DM who had hypertension and microalbuminuria, the ARB drug Irbesartan was found to reduce the risk of

progression to overt nephropathy by 70%[55]. Moreover, in a study in patients with T2DM, ARB reduced urinary albumin excretion by 44%, whereas amlodipine reduced it by only 8%, with essentially the same degree of blood pressure decrease[56].

1.5.2 Glycemic control

The UK Prospective Diabetes Study (UKPDS) and Diabetes Control and Complications Trial (DCCT) demonstrate that controlling blood glucose reduces microvascular complications in people with DN. In addition, DCCT demonstrates that as HbA1c decreases, microvascular complications also gradually decline, with the final indicator approaching the non-diabetic range[57].

Some hypoglycemic drugs have been proven to have an independent protective effect on renal function, in addition to their blood glucose-lowering effects[58]. For instance, peroxisome proliferator-activated receptor gamma (PPARγ) agonists can act nephroprotective against DN independently of their glucose-lowering effects. Meanwhile, several new drugs have been applied in the treatment of T2DM, such as SGLT2 inhibitors (SGLT2i), which reduce glucose reabsorption and lower blood glucose by acting in the kidney, and a growing number of studies have shown that SGLT2i may play a protective role in the kidney[59, 60].

1.6 Sodium-glucose cotransporter 2 inhibitors (SGLT2i)

SGLT2i is a new type of hypoglycemic agent. It lowers blood glucose by reducing the reabsorption of glucose in the kidneys[61]. Since the launch of the

first SGLT2i, dapagliflozin, in 2011, the class has evolved to include empagliflozin, canagliflozin, ertugliflozin, and Tofogliflozin (Table 2). SGLT2 is located almost exclusively in the epithelial cells of the first and second segments of the proximal tubule, where it mediates greater than or equal to 90% of glucose reabsorption (Figure 5)[62]. SGLT1 is expressed on the third segment of the proximal tubule and has a lower glucose reabsorption capacity than SGLT2. SGLT1 is most abundant in enterocytes and mediates the absorption of glucose from the intestinal lumen[63]. To avoid affecting glucose absorption in the intestine, drugs are generally chosen to act on SGLT2 rather than SGLT1. However, Sotagliflozin is an SGLT1 and SGLT2 inhibitor, and Canagliflozin has some inhibitory effect on SGLT1[64, 65].

Hyperglycemia in diabetes is characterized by a greater than normal filtration of glucose from the glomerulus. Furthermore, there is also an increase in glucose concentration in the proximal tubules, and for the reabsorption of this glucose, a compensatory increase in SGLT1 and SGLT2 expression[66]. SGLT2i reduce glucose reabsorption through competitive inhibition, resulting in large amounts of glucose being excreted in the urine[61]. SGLT2i bind to co-transporters with higher affinity than glucose in the tubular lumen of the kidney. Therefore, therapeutic concentrations of SGLT2i can prevent significant reabsorption of glucose. Although SGLT2i cause a decrease in the renal glucose threshold, their hypoglycemic effect diminishes as blood glucose decreases, and therefore do not cause a high risk of hypoglycemia[67].

Table 2. SGLT2i. The table represents the different SGLT inhibitors approved for the treatment of DM (Clifford J, 2022).

Agent	Company	Brand	Dose mg/day	SGLT2 IC$_{50}$ nmol/l	SGLT1 IC$_{50}$ nmol/l
Dapagliflozin	AstraZeneca*	Farxiga	5, 10	1.2	1400
Canagliflozin	Janssen, Napp	Invokana	100,300	2.7	710
Empagliflozin	Boehringer Ingelheim, Eli Lilly	Jardiance	10, 25	3.1	8300
Ertugliflozin	Merck Sharp & Dohme, Pfizer	Steglatro	5, 15	0.9	1960
Sotagliflozin	Lexicon	Zynquista	200	1.8	36
Ipragliflozin	Astellas	Suglat	25, 50	7.4	1875
Luseogliflozin		Lusefi	2.5, 5	2.3	3990
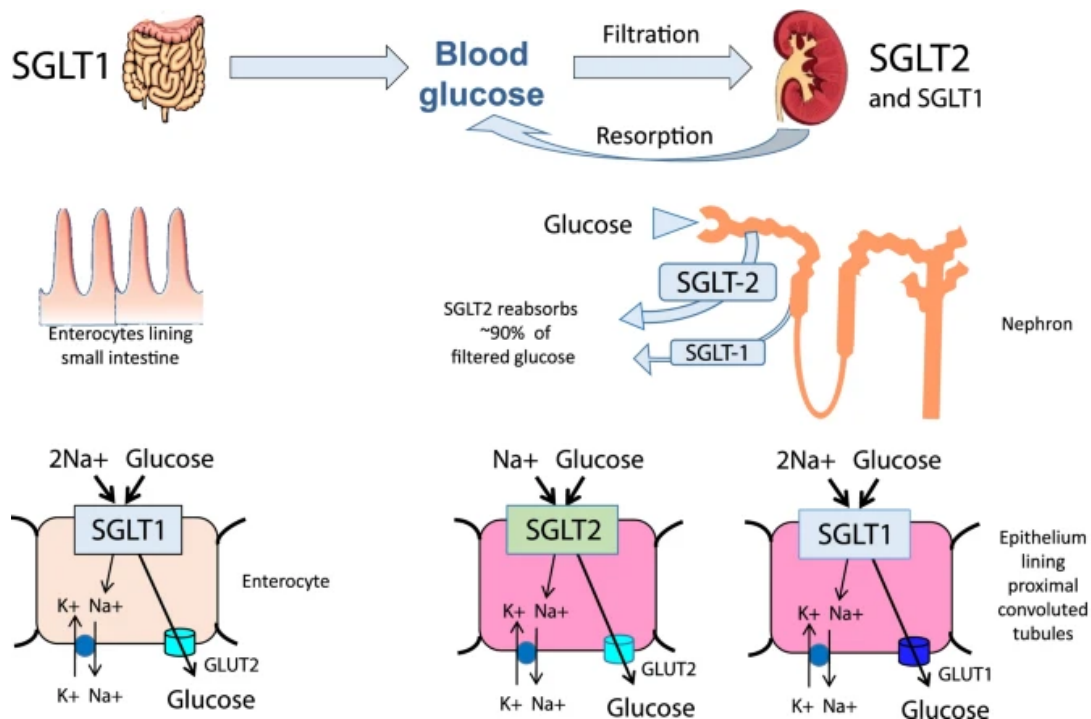
Figure 5. **Key sites of SGLT2i.** SGLT2 is expressed on the first and second segments of the proximal tubule. It mediates most of the glucose reabsorption. SGLT1 is expressed on the third segment of the proximal tubule and has a lower glucose reabsorption capacity than SGLT2, but a higher affinity than SGLT2 to recover the low concentrations of glucose remaining in the tubule (Clifford J,2022).

1.6.1 SGLT2i effects on the kidney

In DN, as SGLT2 and SGLT1 expression increases within the proximal tubules, more glucose is reabsorbed and, along with more sodium, chloride is reabsorbed, thus leading to a decrease in sodium and chloride concentrations in the renal tubular lumen and the macular densa (MD). This decline is in turn mitigated by tubuloglomerular feedback, which increases GFR and partially restores NaCl and fluid excretion[68]. Based on the renal tubule hypothesis, SGLT2 inhibition reduces excessive tubular reabsorption in proximal tubules of DN, thereby alleviating diabetic glomerular hyperfiltration. It was shown that the intra-tubular luminal concentrations of potassium, sodium, and chloride were 25% lower in the diabetic rats compared to the non-diabetic group.

In addition, SGLT2 inhibition, either genetically or pharmacologically, reduces the glomerular hyperfiltration reactions in diabetic mice[69, 70]. The use of short-term SGLT2 inhibition reduces GFR and has been demonstrated in humans[71]. In studies of patients with T2DM, three large clinical trials have found that SGLT2i including dapagliflozin, empagliflozin, and canagliflozin, in addition to lowering the incidence of heart failure, also reduced the hazard ratio for eGFR and had a protective effect on the kidneys[72-75]. The Clinical Evaluation of Renal Disease (CREDENCE) trial provides the first evidence of slowing the progression of DN in T2DM treated with Canagliflozin[76]. Therefore, FDA grants approval for canagliflozin to treat DN based the CREDENCE trial. Moreover, the Dapagliflozin and Prevention of Adverse Outcomes in Chronic Kidney Disease (DAPA-CKD) trial proved that the Dapagliflozin improved the prognosis of patients with chronic kidney disease (CKD) regardless of the existence of T2DM[77]

1.6.2 Renoprotection pathways of SGLT2i

Current studies have identified potential protective mechanisms for the kidney with SGLT2i including reducing glomerular hypertension and hyperfiltration, promoting antifibrosis and anti-inflammation, and reducing body weight and blood pressure (Figure 6)[78, 79]. Experimental models of T1DM and T2DM found that SGLT2i reduced inflammation, oxidative stress, and fibrosis[80, 81]. SGLT2i were found to reduce structural damage to renal tubules and glomeruli in different animal models[66, 82].

Furthermore, SGLT2i may also improve renal hypoxia in diabetes. In diabetics, due to their increased glucose transport to the proximal tubule, more oxygen is

utilized for energy to reabsorb the increased glucose, resulting in renal hypoxia[83, 84]. Although the mechanisms underlying the molecular protection of SGLT2i in the kidney have not been fully elucidated, their effects on hemodynamics are relatively well understood. It has been demonstrated in animal models that SGLT2i can reduce T1DM hyperfiltration[85-87]. In addition to the renoprotective effects of SGLT2i found in the CANVAS Program and EMPA-REG OUTCOME trials, several clinical trials have found that SGLT2i reduce urinary protein excretion in patients with diabetic nephropathy[88, 89]. In addition, SGLT2 inhibition reduced levels of inflammation, markers of renal tubulointerstitial disease, and tubular injury.
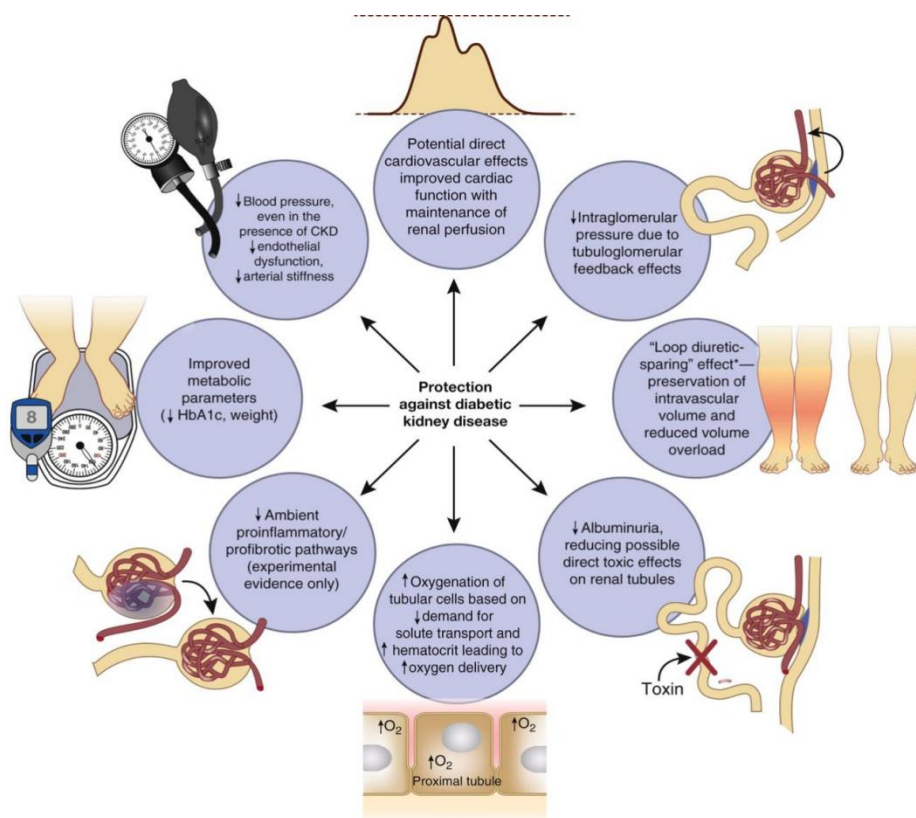
Figure 6. Potential mechanisms for inhibition of SGLT2 renal protection (Hiddo J L, 2018).

1.7 Objectives of the study

Recently, it was found that SGLT2i provides additional renoprotective effects beyond ARB. However, the underlying molecular mechanisms of the renoprotective effects of SGLT2i have not been completely elucidated. Therefore, exploring the molecular mechanisms behind SGLT2i that protect the kidney will help us optimize therapies for patients with DN.

The main objective of this project is to explore the renoprotective mechanism associated with SGLT2i in DN and whether there is additional renoprotection when ARB and SGLT2i are combined. We used BTBR ob/ob mice as a model for type 2 diabetic model with DN, which is very similar to early human DN. We performed experiments on the mouse model over 12 weeks, assessing variables such as in body weight, blood glucose, urine albumin-to-creatinine ratios (UACR), kidney weight/body weight ratio (KW/BW%), and representive Periodic Acid Schiff (PAS) staining of kidney tissues. As a result, BTBR ob/ob mice exhibit the primary clinical and histologic characteristics of DN, including hyperglycemia, proteinuria, progressive loss of renal function, and glomerulosclerosis. Treatments of SGLT2i and/or ARB attenuated the above characteristics of DN.

While mouse models of diabetic nephropathy (DN) are valuable, they are also limited in their capacity to faithfully represent the complete spectrum of DN phenotypes to varying degrees. Therefore, we combined single nucleus RNA sequencing (snRNA-seq) with the mouse model. snRNA-seq can describe cell types, health, disease states, and construct detailed cellular profiles. Furthermore, snRNA-seq offers an unbiased and powerful method for uncovering the kidney's responses during the progression of DN and understanding how different treatment can prevent the deterioration of the

condition. This study aimed to explore the molecular and cellular drivers of DN and the specific response of renal cells to SGLT2i by snRNA-seq.

2. Materials and Methods

2.1 Materials

2.1.1 Equipments

Table 3. Equipments

Equipments	Manufacturer
Sartorius Practum analytical balance	MS Laboratory Equipment, Heidelberg
Tecan Sunrise	Fornax Technologies, GmbH
Roller mixer	CAT, Ballrechten-dottingen
Centrifuge 5810	Eppendorf AG, Hamburg
Centrifuge 5910R	Eppendorf AG, Hamburg
Centrifuge 5424R	Eppendorf AG, Hamburg
Centrifuge 5810R	Eppendorf AG, Hamburg
C1000 touch thermal cycler	Bio-Rad Laboraties, Munich
Pipettes (2 µl,10 µl, 20 µl, 200 µl, 1000 µl)	Eppendorf AG, Hamburg
Microscope ECLIPSE Ts2	Nikon, Tokyo
Test tube shaker	Heidolph, Schwabach
Open Heating Bath	Julabo, GmbH

2.1.2 Consumables

Table 4. Consumable products

Consumable products	Manufacturer
Pipette Tips (10 µl,20 µl, 200 µl, 300 µl ,1000 µl)	Sarstedt AG&Co, Nümbrecht
Serological Pipette (2 ml, 5 ml, 10 ml)	Sarstedt AG&Co, Nümbrecht

Micro tubes (1.5 ml, 2 ml)	Sarstedt AG&Co, Nümbrecht
Centrifuge Tubes (15 ml, 50 ml)	Greiner Bio-One, Frickenhausen
Syringe Needle 24G	Becton Dickinson, Heidelberg
Injekt®-F syringe (1 ml)	B. Braun Melsungen AG, Melsungen
KIMBLE Dounce tissue grinder set	Sigma-Aldrich, Deisenhof
CellTrics Filters (5 µm, 30 µm)	Sysmex, Norderstedt
Biosphere Filter Tips 1250 µl extra long	Sarstedt AG&Co, Nümbrecht
Razor blade	Dahlhausen, Cologne
Petri dish (30 mm)	Thermo Fisher Scientific, Rockford
Polystyrene Conical tube (15 ml)	Th. Geyer，Renningen

2.1.3 Reagents

Table 5. Reagent for urine Albumin ELISA

Chemical product	Manufacturer
Carbonate-Bicarbonat, pH 9.6 (0.05M)	Sigma-Aldrich, Deisenhof
Tris Buffered Saline, with BSA, pH 8.0 (50mM)	Sigma-Aldrich, Deisenhof
TBS, 1%BSA, pH 8.0, 0.05% Tween20 (50mM)	Sigma-Aldrich, Deisenhof
Tris Buffered Saline, with Tween® 20, pH 8.0 (50mM)	Sigma-Aldrich, Deisenhof
TMB One Component Substrate	Biomol, Hamburg
2N H_2SO_4	Merck, Darmstadt
10% Tween 20	Biomol, Hamburg

Table 6. Reagent for PAS staining

Chemical product	Manufacturer

Schiff's reagent	Merck, Darmstadt
Hematoxylin	SERVA, Heidelberg
Periodic acid	Carl Roth, Karlsruhe
Sodium iodate	Avantor, Pennsylvania
Hydrochloric acid 25%	Merck, Darmstadt
Potassium aluminum sulfate dodecahydrate	Sigma-Aldrich, Deisenhof

Table 7. Reagent for isolation of single nuclei

Chemical product	Manufacturer
SUPERaseIN RNAse Inhibitor (20 U/µl)	Thermo Fisher Scientific, Rockford
RNAsin Plus(40U/µl)	Promega，Madison
RNAlater	Thermo Fisher Scientific, Rockford
UltraPure^{TM}BSA Non-Acetylated	Thermo Fisher Scientific, Rockford
Red blood cell lysing buffer hybri-max^{TM}	Sigma-Aldrich, Deisenhof
Dulbecco's Phosphate Buffered Saline	Sigma-Aldrich, Deisenhof
Calcium Chloride Solution 2.5M	Jena Bioscience, Jena
EDTA Solution 0.5M pH 8.0	Jena Bioscience, Jena
Tris-HCl Buffer 1M pH 8.0	Jena Bioscience, Jena
Saccharose	Merck, Darmstadt
Magnesiumacetat-Lösung	Merck, Darmstadt
Triton X-100 Lösung	Merck, Darmstadt

Table 8. Antibodies for histology

Antibody	Manufacturer
Mouse Albumin Polyclonal Antibody	Thermo Fisher Scientific, Rockford
Anti-Mouse Albumin, HRP conjugated	Biomol, Hamburg

2.1.4 Buffers

Table 9. Buffer for urine Albumin-Elisa

Buffer	Components	Volume/Quality
Coating buffer	Carbonat-Bicarbonat pH 9.6	5 mol
	dH$_2$0	100 ml
Postcoat buffer	0.1% BSA, Tris pH8.0	50 mmol
	dH$_2$0	1 L
Sample Diluent	10% Tween 20	250 µl
	Postcoat Buffer	50 ml
Washing buffer	Tris,0.05% Tween 20	50 mmol
	dH$_2$O	1 L

Table 10. Buffer for PAS staining

Buffer	Components	Volume/Quality
1% Periodic Acid	Periodic acid	2 g
	dH$_2$0	200 ml
HCL-Alcohol	25% HCl	2 ml
	100% Ethanol	200 ml
Hematoxylin	Potassium aluminum sulfate dodecahydrate	12.5 g
	Sodium iodate	0.125 g
	dH$_2$O	250 ml
	Hematoxylin powder	1.25 g
	Ethanol	12.5 g

Table 11. Lysis buffers for isolation of single nuclei

Lysis buffer	Components	Volume
Nuclei Lysis Buffer 1	1M Tris pH8	0.5 ml

	1M sucrose	8 ml
	2.5M CaCl$_2$	50 µl
	1M MgAc2	75 µl
	0.5M EDTA	5 µl
	dH$_2$O	16.37 ml
Nuclei Lysis Buffer 2	Nuclei Lysis Buffer 1	4845 µl
	1M DTT	5 µl
	10% TritonX-100	50 µl
	20 U/µl SUPERaseIN RNAse Inhibitor	50 µl
	40 U/µl RNAsin Plus RNAse Inhibitor	50 µl
Resuspension buffer	PBS	1580 µl
	50 mg/ml BSA	400 µl
	40 U/µl RNAsin Plus RNAse Inhibitor	20 µl
Rinsing buffer	PBS	4900 µl
	0.1% BSA	100 µl
Washing buffer	PBS	4975 µl
	50 mg/ml BSA	10 µl
	20 U/µl SUPERaseIN RNAse inhibitor	10 µl
	40 U/µl RNAsin Plus RNAse Inhibitor	5 µl

2.1.5 Kits

Table 12. Kits

Product name	Manufacturer
Chromium Next GEM Single Cell 3' GEM, Library & Gel Bead Kit v3.1, 4 rxns	10X Genomics, Pleasanton
Creatinine Jaffé Gen.2 kit	Roche, Basel

2.2 Methods

2.2.1 Mouse diabetic kidney disease models

All animal protocols comply with the National Institutes of Health's Guide for the Care and Use of Laboratory Animals and the German Animal Welfare Law. Mice were housed in an animal facility free of specific pathogens with free access to feed and water and a 12-hour light-dark cycle, Strict standard procedures for breeding and genotyping were followed. Hamburg BGV government approved animal experiments. Wild type mouse BTBR (Jax No 002282), heterozygotes BTBR ob/+(BTBR.Cg-Lep$^{ob/wt\ WiscJ}$) (Jax No. 004824) and Podocyte-reporter mouse (Gt (ROSA)26Sor$^{tm4(ACTB-tdTomato,\ -EGFP)\ Luo}$; Tg (NPHS2-cre)^{295Lbh}) (Jax No. 007576) were purchased from JAX (Bar Harbor, Maine, USA). Podocyte-reporter mice were crossed with BTBR wild-type animals for at least 7 generations before BTBR. Cg-Lep$^{ob/wt\ WiscJ}$; Gt (ROSA)26Sor$^{tm4(ACTB-tdTomato,\ -EGFP)\ Luo}$; Tg (NPHS2-cre)^{295Lbh} animals were generated. The resulting progeny were then crossed to obtain Gt (ROSA)26Sor$^{tm4(ACTB-tdTomato,\ -EGFP)\ Luo}$; Tg (NPHS2-cre)^{295Lbh}; BTBR.Cg-Lep$^{ob/ob\ WiscJ}$ and Gt (ROSA)26Sor$^{tm4(ACTB-tdTomato,\ -EGFP)\ Luo}$; BTBR.Cg-Lep$^{wt/wt\ WiscJ}$; Tg (NPHS2 -cre) ^{295Lbh} mouse.

2.2.2 Animal groups

The following five groups of male and female mice were studied (average number of males and females): 1) The control group was wt mice with no therapeutic intervention, n=6; 2) The control group was BTBR ob/ob mice with no therapeutic intervention, n=11; 3) BTBR ob/ob mice were treated with empagliflozin as food at a dose of 50 mg/kg/d at 8 weeks of age, n=8; 4) BTBR ob/ob mice were treated with losartan at a concentration of 100 mg/L in drinking

water, n=8; 5) BTBR ob/ob mice were treated with both losartan and empagliflozin, n=8. All treatments started at 8 weeks of age and lasted for 12 weeks.

2.2.3 Tissue handling

Mice were anesthetized with 180 mg/kg of ketamine and 16 mg/kg of xylazine in 0.9% NaCl by intraperitoneal injection, and after collecting blood the mice were executed by decortication. Sprayed the abdominal fur of mice with 70% ethanol before opening the abdominal cavity. The right and left kidneys were removed, and each kidney was weighed. Each kidney was cut horizontally with a knife and divided into 5 parts. The top parts of each kidney were placed in the RNAlater for snRNA-seq. Two sections were placed in 4% paraformaldehyde and one in liquid nitrogen for histological examination. The bottom parts of each kidney were placed in a cryostor, placed at -80 degrees for gradient cooling, and then stored for later histological analysis.

2.2.3.1 Extraction of blood serum

Fresh blood samples were collected before the start of treatment and the experimental endpoint. Fresh blood samples were transferred to EDTA tubes and placed at room temperature for 10-30 minutes. The supernatant was then extracted by centrifugation at 1500g for 10 min and then centrifuged at 1500g for another 10 min. Finally, transferred the supernatant to a 1.5 ml Eppendorf tube and store at -20°C until analyzed.

2.2.3.2 Urine collection

Urine collection was obtained at the start of treatment and 2-week intervals until the end of the study. Assessment of proteinuria in urine samples using the ratio of albumin to creatinine. The urine samples were centrifuged at 2000g for 10 minutes and the supernatant was taken for albumin and creatinine measurements.

2.2.4 Blood and urine diagnostics

2.2.4.1 Hematochemistry

Non-fasting blood glucose was measured every 2 weeks with the blood glucose meter (Accu-Chek Aviva, Roche) to monitor blood glucose level started at 8 weeks of age.

2.2.4.2 Albumin and creatinine analysis in urine samples

In Table 8 and Table 9, all buffers and reagents used to detect albumin in urine were summarized and all solutions need to be recovered to room temperature before use. Prepared dilutions according to Tables 13 and 14, adjusted the urine samples to the appropriate protein concentrations.

Table 13. Dilution of urine for albumin-ELISA

Urine-Stix	Trace or +	++	+++
Dilution	1:100	1:1000	1:10000

Table 14. Adjustment of urine samples for working concentrations

Final Dilution	Diluted stock I Stock S/D	Diluted stock II Stock I S/D	Diluted stock III Stock II S/D
1:100	4 µl +396 µl		
1:1000		40 µl +360 µl	
1:10000			40 µl +360 µl

Stock = Urine

S/D = Sample/Diluent Buffer

First, the anti-mouse albumin antibody was coated on high binding power 96-well plates, transferred 100 µl coating buffer to each well (anti-mouse albumin antibody: coating buffer = 1:100), and then sealed the 96-well plate with a sealing membrane. Incubated the plate overnight at 4°C. The next day removed the coated buffer and wiped the plate with a paper towel. Washed 3 times with washing buffer 200µl/well and removed the washing buffer and blot the plate carefully onto paper towels. To block the point of open bonding, 150µl of postcoat buffer was added to each well and incubated for 30 minutes at RT with a shaker. Removed the postcoat buffer and blot the plate onto paper towels, washed 3 times with washing buffer 200µl/well. Removed the washing buffer and blot the plate carefully onto paper towels. Next, prepare the dilutions of samples and standards (Concentrations listed in Table 15).

Table 15. Adjustment of protein standards for working concentrations

For 1 plate	Concentration [ng/ml]	Calibrator	Sample Diluent
Stock solution:	1,000,000	2 µl	198 µl
Standard 1	1000	100 µl Stock solution	900 µl

Standard 2	500	300 Standard 1	300 μl
Standard 3	250	300 Standard 2	300 μl
Standard 4	125	300 Standard 3	300 μl
Standard 5	62.5	300 Standard 4	300 μl
Standard 6	31.25	300 Standard 5	300 μl
Standard 7	15.625	300 Standard 6	300 μl
Blank	BL	--	300 μl

added 100μl/well of standards, blanks, and samples. Incubated on a shaker for 1 hour at room temperature. The plates were washed five times with washing buffer at the end of the incubation time. To detect proteins, HRP conjugated anti-mouse albumin antibody diluted 1:40 000 and added to plate 100μl/well. 1-hour incubation in the dark at room temperature with mild shaking. The plates were washed five times with wash buffer. Add 100μl/well of TMB substrate in the dark. After 3 minutes, stop the reaction by adding 100 μl/well stop solution and evaluate the plate within 30 minutes. Color intensity was calculated at OD_{450nm} with the ELISA reader.

To detect creatine in the urine, the samples were diluted in 1:2 with ddH_2O and used the creatinine Jaffé Gen.2 kit. The measurements were performed under the manufacturer's recommendation.

2.2.5 Histology

2.2.5.1 Fixation of tissue samples

The kidney cuts were kept overnight in 4% paraformaldehyde, tissues were washed four times with PBS at room temperature for 30 minutes each to remove paraformaldehyde. Next, the tissue was placed in the embedding cassettes in PBS overnight at 4 °C.

2.2.5.2 Preparation of histological samples

The embedding cassettes were placed in 50% ethanol at room temperature and preserved for 2.5 hours. First, the tissues were dehydrated by transferring them sequentially into ethanol at 60%, 70%, 96%, and 100% concentrations. Then, after transferring the tissue into Xylol, then into paraffin. This process took approximately 17 hours. Finally, the tissues were embedded in paraffin.

2.2.5.3 Sample slice processing

Tissues were cut into thin slices of 1.5-μm thickness. Before PAS staining of the tissues, paraffin was first removed from the tissues, followed by hydration, and finally washed with distilled water (Table 16).

Table 16. Tissue de-paraffinization, hydration, and washing.

Step	Ingredient	Incubation time（**Minute**）
1	100% Xylol	5
2	100% Xylol	5

3	100% Xylol	5
4	100% EtOH	5
5	100% EtOH	5
6	100% EtOH	5
7	96% EtOH	5
8	96% EtOH	5
9	70% EtOH	5
10	70% EtOH	5
11	dH_2O	5
12	dH_2O	5
13	dH_2O	5

2.2.5.4 Periodic acid Schiff stain

1.5 µm thick 4% PFA fixed paraffin-embedded kidneys were sectioned. PAS-stained solutions were all brought back to room temperature and the staining process was carried out at room temperature. The tissues were degreased and rehydrated. Next, tissues were then stained by placing them in 1% periodic acid solution for 15 minutes. After staining, place them in running water for 3 minutes. Transferred the tissues to a cuvette filled with Schiff's reagent for 1 hour and put them in warm running water for 7 minutes, then rinsed with distilled water. The core was stained with Hematoxylin solution for 1-3 minutes and in running tap water for 2 minutes.

Next, the slides were quickly placed into hydrochloric acid (HCl/EtOH) solution 3 times for 3 seconds each. After that the tissues were put into 70% ethanol for one minute, then 96% ethanol 2 times for 2 minutes each, 100% ethanol 3 times the first time for 2 minutes the second time for 5 minutes the third time for 10

minutes, and finally into 100% xylene 2 times for 5 minutes each. Finally, the tissues were coated with Entellan mounting medium and sealed with a 60 mm cover glass.

2.2.6 Single nuclei preparation

Started with a small (1-2 mm) piece of kidney tissue stored in RNAlater at -20°C and placed on a 30 mm dish. Added 100 µl of lysis buffer to the 30 mm dish and minced the biopsy with a fresh razor blade. Next, added another 100 µl lysis buffer to the minced tissue and transferred it into a Dounce tissue grinder. Ground the minced tissue 30 times with a loose pestle (A) and ground the homogenate 30 times with a tight pestle (B), respectively.

To reduce heat caused by friction, homogenization should be performed gently on ice. Transferred the solution to a 15 ml low-binding tube. Washed the dounce with 800 µl lysis buffer and transferred it to the 15 ml Falcon. Added another 3 ml of lysis buffer to the 15 ml Falcon to make the total volume 4 ml. Then, mix and incubated the solution for 30 min on ice. During incubation, homogenize every 5 minutes with a 1250 µl pipette tip and take 20 µl homogenate every 10 minutes to observe under the microscope. Passed the homogenate through a 30 µm strainer into a new 15 ml low-binding Falcon. Rinsed the strainer with the remaining 1ml lysis buffer. Centrifuged the Falcon at 500g for 5 min at 4℃ (Centrifuge setting is accel/brake 5). Removed the supernatant with a glass Pasteur pipette and remained the pellet.

Next, resuspended the pellet with 1 ml 0.01% BSA. Rinsed a new 15 ml Falcon with 1mg/ml BSA to wet the inner surface of the Falcon and shake out the BSA remaining at the bottom of the Falcon. Passed the nuclei suspension through a

33

5 μm strainer into the BSA-coated 15 ml low binding Falcon, rinsed the strainer with 1 ml 0.01%BSA, and added additional 3 ml of 0.01%BSA for a total volume of 5 ml. Centrifuged the Falcon at 500 g for 5 min at 4℃. Removed the supernatant using a Pasteur pipette and lab vacuum. Then, resuspended the pellet in around 200 μl 1%BSA. Finally, prepared 10x chip loading, which can be diluted further if needed before loading.

2.2.7 Data analysis of snRNA-seq

SnRNA-seq was performed by Beijing Genomics Institute; the data analysis was performed by Tianran Zhang using the Seurat package based on R programming software.

2.2.7.1 Pre-processing and quality control

To start the analysis of snRNA-seq data, we used the raw data generated from 10x Genomics, and the gene-cell count matrix was obtained using Cell Ranger software (version 5.0.1). Each sequencing read assigned to the corresponding cell barcode was compared to the reference genome (using the 10× Genomics mouse genome mm10s) to count the genes in each cell with a unique molecular identifier (UMI).

We then performed a quality control (QC) step to ensure that the data for each cell barcode corresponded to a high-quality cell. While low-quality cells include damaged cells, dying cells, and multiple cells sharing a single barcode (doublets). We first removed possible ambient RNA contamination by using soupX[90]. Then, we kept the nucleus with more than 500 and less than 6000 genes detected and no more than 2% of mitochondrial genes detected.

Furthermore, a scrublet was applied to remove potential doublets[91].

2.2.7.2 Normalization and integration

After performing quality control, normalization was required to make the snRNA-seq data comparable between samples. Two common methods for normalizing snRNA-seq data were log-normalization and probabilistic model-based approach. In our study, we used log-normalization. First, we applied the size factor of 10,000 to scale the gene count matrix. Then the log transformation was performed to reduce distributional skewness. As a result, the normalization step increased the power of low-expressed genes when performing differential gene expression analysis, making downstream analyses more accurate and easier[92].

To remove unwanted technical variance between different batches. In our data, we used the Seurat integration method[93]. The Seurat integration method identifies highly variable genes (HVGs) in each dataset after first normalizing each dataset separately. The data scaling process then used the highly variable genes, and each dataset's expression values were normalized and centered.

Before that, we identified the highly variable genes for each sample separately which can help reduce bias and highlight biological signals. Features showing repeatedly variables across samples were selected for integration. The integrated data assay was then created by the "FindIntegrationAnchors" and "IntegrateData" functions.

2.2.7.3 Dimensionality reduction and clustering

Dimensionality reduction is a critical step in snRNA-seq data analysis and includes both non-linear and linear methods.

First, we performed PCA and then applied UMAP on the PC space. The number of principal components (PCs) used was determined according to the percentage of variance explained by the components. For our data, the first 30 PCs were used.

We generated different cell clusters with the function FindClusters by different resolutions. Then we chose 0.3 as the final resolution used for clustering and later annotation because of their biological separation. The results of clustering were visualized using UMAP. The marker genes for each cluster were determined by the FindAllMarkers function with the Wilcoxon rank sum test. We compared each cluster's top marker genes to the publicly known marker genes for kidney cell types to annotate the cell clusters with cell type names.

2.2.7.4 Downstream analysis

Further downstream analysis was performed to discover and interpret the biological differences between conditions of each cell type. The three primary downstream analysis methods used in this study are differential gene expression (DEG) analysis, transcription factor analysis, and cell-cell communication analysis.

We currently performed DEG analysis, which involves identifying genes that are differentially expressed under different circumstances, and this information can help us gain insight into the underlying molecular mechanisms of cell differentiation or disease pathogenesis.

2.2.7.4.1 Differentially expressed genes for conditions

By applying DEG analysis, we compared different experimental conditions in specific cell clusters. We used the Wilcox test from the Seurat package and genes with adjusted p-value < 0.05 and |log2FC| > 0.25 were identified as significantly differentially expressed between conditions.

2.2.8 Statistical analysis

Data were analyzed using GraphPad Prism version 9 using the unpaired t-test and one-way ANOVA test, as shown in Table 17.

Table 17. Definition of significance.

Significance grade	Symbols
Not significant	ns
*	P < 0.05
**	P < 0.01
***	P < 0.001
****	P < 0.0001

3. Results

3.1 Characterization of SGLT2i and/or ARB-treated DN mice

3.1.1 Treatment using SGLT2i and/or ARB

Treatment was started when the BTBR ob/ob mice were 8 weeks old and continued for 12 weeks. BTBR ob/ob mice were divided into five groups: 1. WT control; 2. vehicle-treatment control; 3. treatment with SGLT2i (empagliflozin); 4. treatment with ARB (losartan); 5. combined treatment with SGLT2i and ARB. Various clinical parameters were measured at different time points to monitor treatment efficacy and to monitor the renal function. At the end of treatments, kidneys were collected and used for morphological analysis and snRNA-seq (Figure 7).
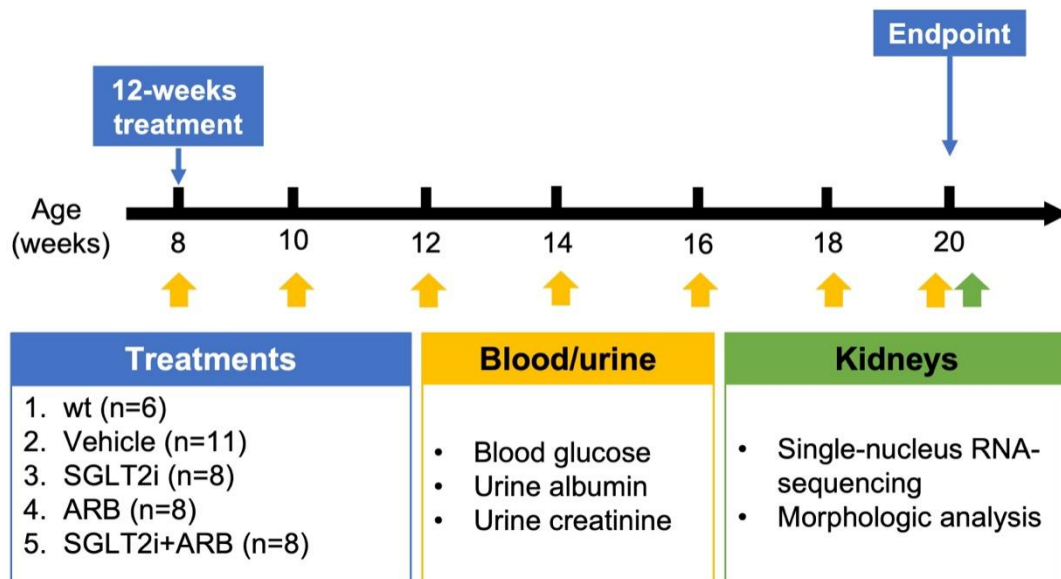

Figure 7: Experimental scheme: Blood glucose was measured, and urine was collected for monitoring for every 2 weeks. The treatment was started at 8 weeks of age. All mice were sacrificed after 12 weeks of treatment.

3.1.2 Body weight

We used BTBR ob/ob and BTBR wt mice to study the molecular and cellular changes regarding DN. At 8 weeks old, BTBR ob/ob mice already show obesity in both males and females compared to wt mice. The ob/ob mice have significantly higher body weight than wt mice, while no significant difference in body weight was found between groups of ob/ob mice during the treatment (Figure 8).
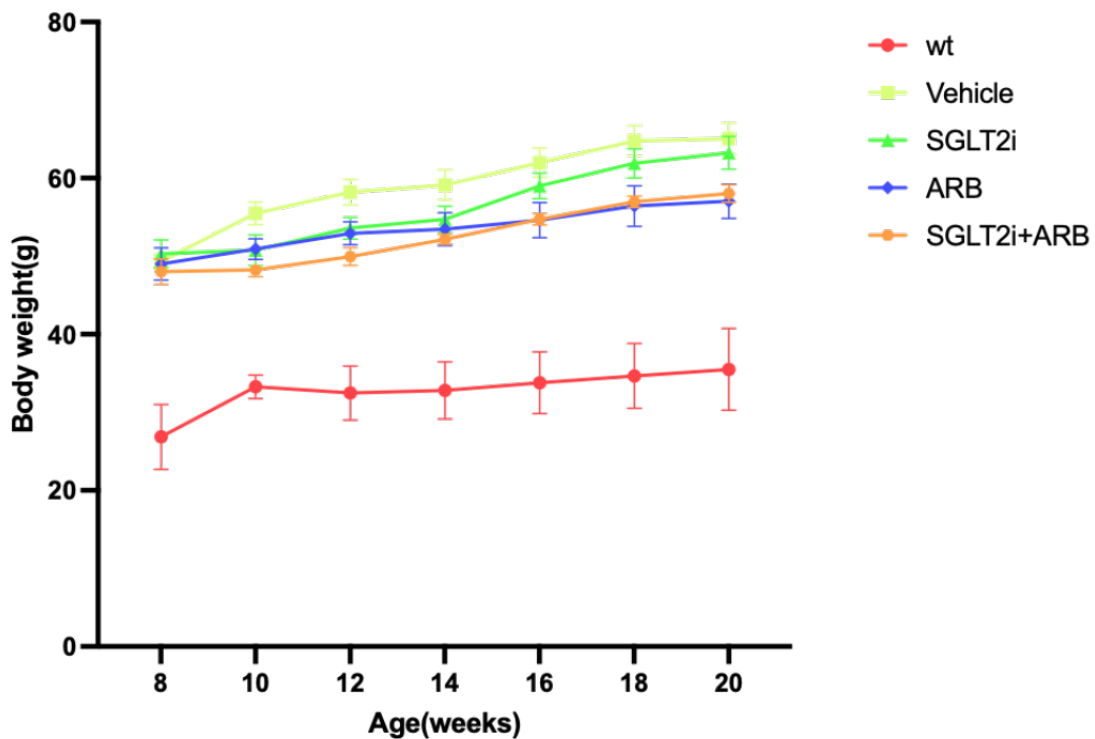

Figure 8: Weight of mice after 12 weeks of treatment.

3.1.3 Non-fasting blood glucose

BTBR ob/ob mice had hyperglycemia. Treatment of SGLT2i significantly lowered the non-fasting blood glucose toward the normal value. Interestingly, we found that SGLT2i was more effective in lowering blood glucose than SGLT2i+ARB (Figure 9).
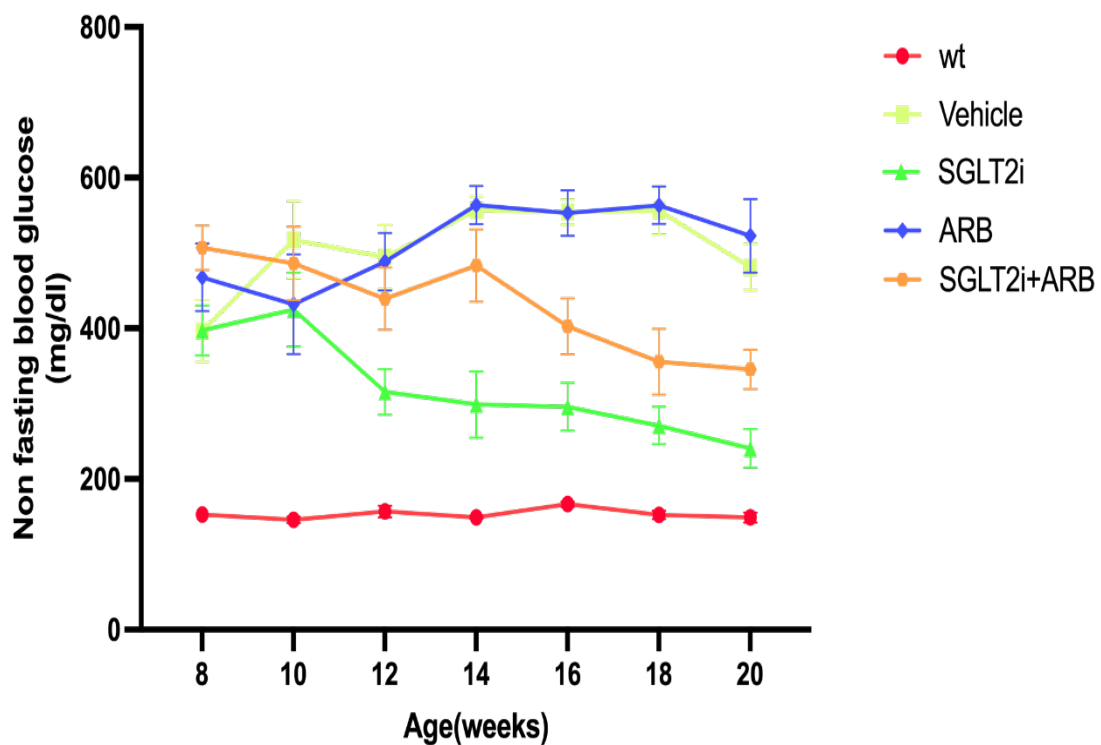

Figure 9. Non-fasting blood glucose of mice after 12 weeks of treatments. Non-fasting blood glucose levels after 12 weeks of treatment with different drugs, with week 8 indicating baseline values before the start of treatment.

3.1.4 Kidney weight/body weight ratio

Compared with wt mice, Vehicle, ARB-treated, and SGLT2i+ARB-treated ob/ob mice had reduced KW/BW%, while no significant difference in KW/BW% was observed in SGLT2i-treated group (Figure 10).
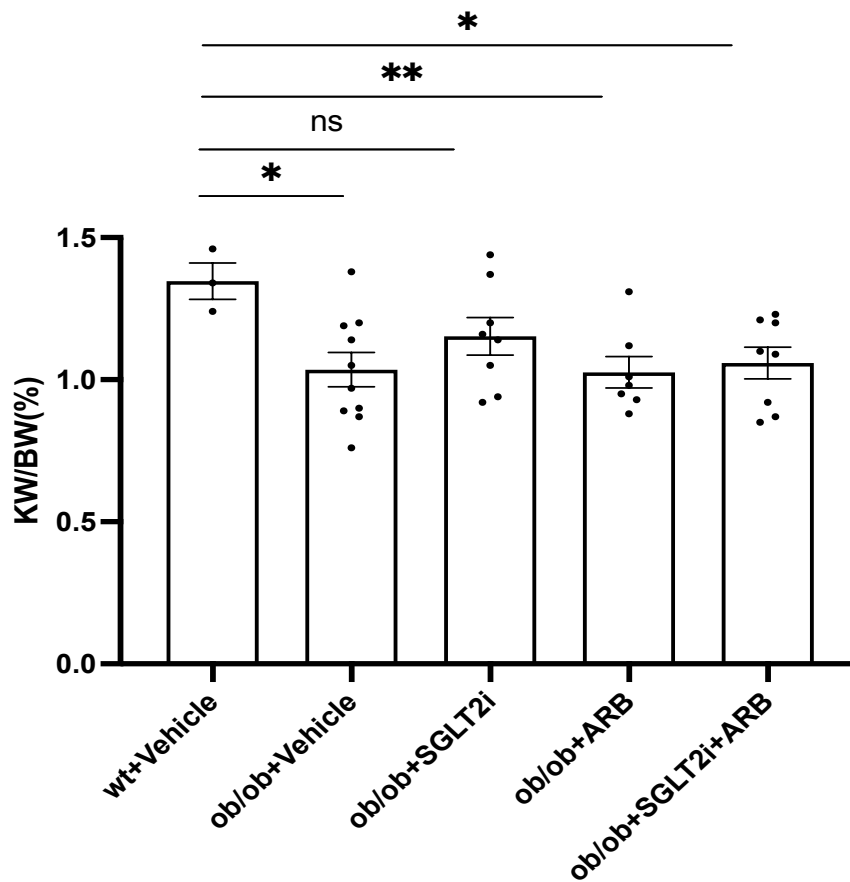

Figure 10. Kidney weight/body weight ratio. KW/BW% of BTBR wt controls compared to BTBR ob/ob mice (*$P < 0.05$, **$P < 0.01$, ns, not significant, unpaired t-test).

3.1.5 Urine albumin-to-creatinine ratios

UACR were increased in ob/ob mice compared to wt mice, but a significant decrease in UACR was found in all drug-treated groups (Figure 11).
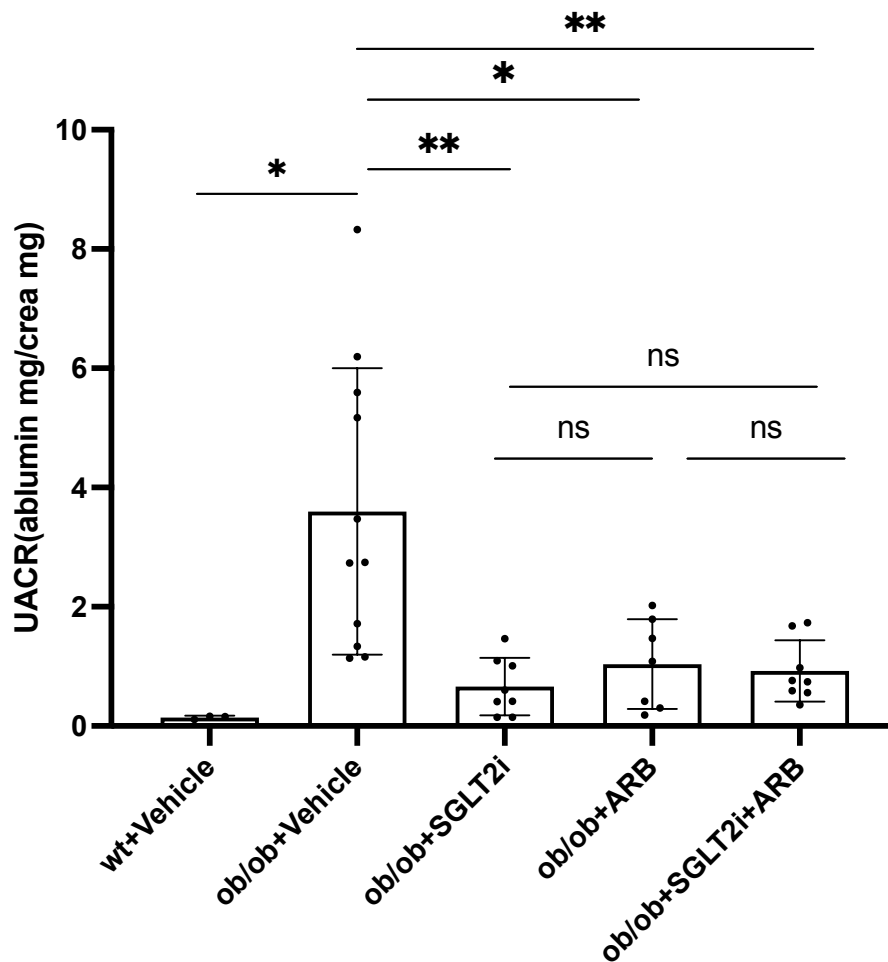

Figure 11. Urine albumin-to-creatinine ratios. UACR of BTBR ob/ob mice compared to BTBR wt controls and BTBR ob/ob mice were compared under different treatment conditions (*P < 0.05, **P < 0.01, ns, not significant, unpaired t-test).

3.1.6 PAS staining

In PAS staining, increased mesangial expansion and larger glomerular volumes were seen in ob/ob mice compared to wt mice but decreased in all treatment groups, most especially in the SGLT2i+ARB treatment group (Figure 12).
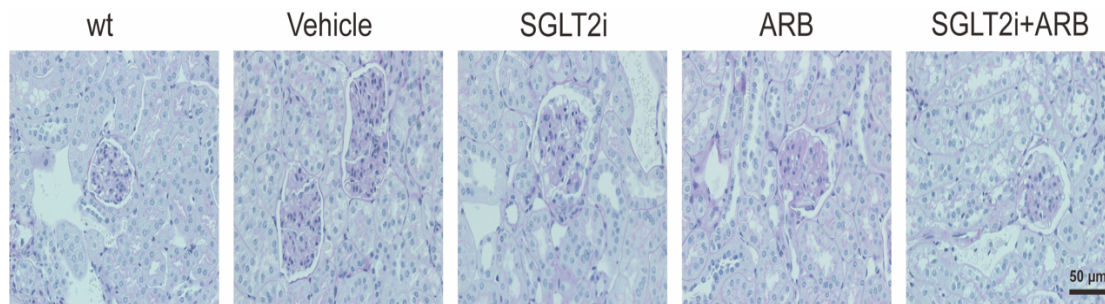

Figure 12. PAS staining changes after 12 weeks of treatments. Images of PAS-stained kidney sections from wt mice or BTBR ob/ob 12 weeks after treatment. Original magnification: ×400.

3.2 The data of snRNA-seq

3.2.1 Overview of the murine kidney preparation protocol used for snRNA-seq

Kidney tissues were extracted from a total of 5 female mice at 20 weeks of age, including one mouse from each of the following 5 groups: 1. WT control; 2. vehicle-treatment control; 3. treatment with SGLT2i; 4. treatment with ARB; 5. combined treatment. Nuclei were extracted from selected kidney tissues and analyzed using 10x Genomics Chromium next GEM single cell 3' Reagent Kit v3.1(Figure 13).
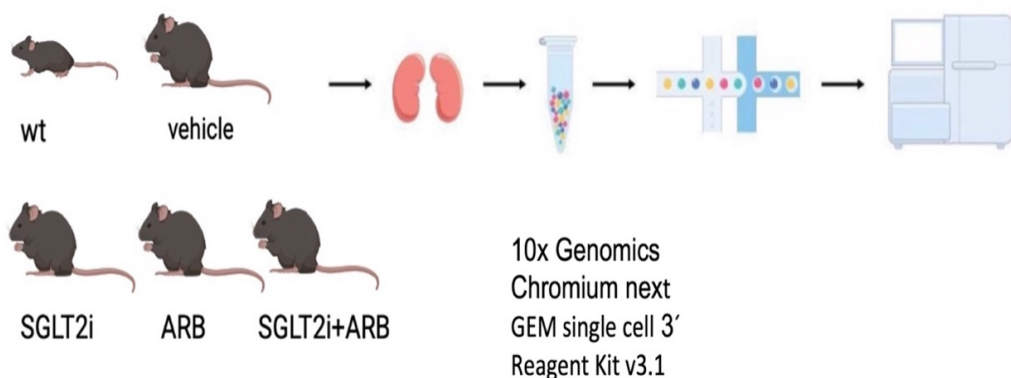
Female, n=1 per condition

Figure 13. Overview of the murine kidney preparation protocol used for snRNA-seq.

3.2.2 Quality control for the snRNA-seq

In addition to the analysis mentioned earlier, we took further measures to ensure the accuracy of our results. We performed quality control for the number of genes detected in each cell type and checked the quality of single nuclei by monitoring the percentage of ribosomal and mitochondrial genes. This quality control step helped us ensure that the cells included in our analysis were of high quality and that any observed changes in gene expression were not due to technical artifacts. By carefully controlling for these factors, we increased the reliability and reproducibility of our results (Figure 14).
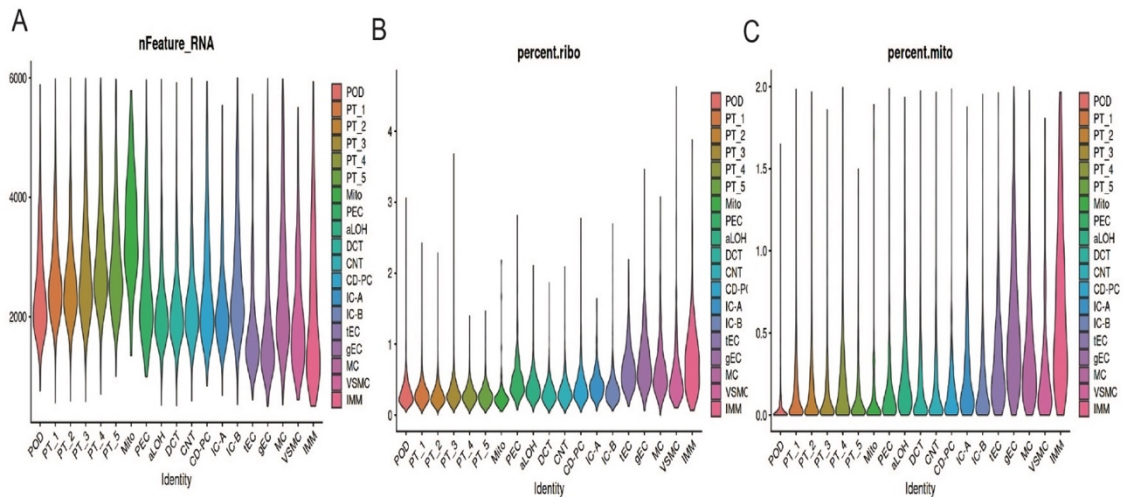
Figure 14. Quality control for the snRNA-seq. (A) the number of genes detected in each cell type. The percentage of ribosomal (B) and mitochondrial (C) genes as a sign of cell conditions.

3.2.3 Cell type annotation in UMAP plot

After completing data pre-processing and quality correction, 51767 single cells in total were analyzed. Cells in the 19 clusters were categorized into 19 cell types and annotated according to the reported kidney cell-specific marker genes (Figure 15).

Figure 15. Annotated cell type UMAP plot. UMAP plot for 51767 cells from all kidney samples (n=5) demonstrating 19 cell types. Abbreviations: PT, proximal tubule; aLOH, ascending loop

of Henle; DCT, distal convoluted tubule; CNT, connecting tubule; CD-PC, collecting duct principal cell; tEC, tubule epithelial cells; gEC, glomerular epithelial cells; IC-A, alpha intercalated cell, IC-B, beta intercalated cell; MC, mesangial cells, VSMC, vascular smooth muscle cells; POD: podocyte; PEC, parietal epithelial cell; Mito, mitotic cell; IMM, immune cell.
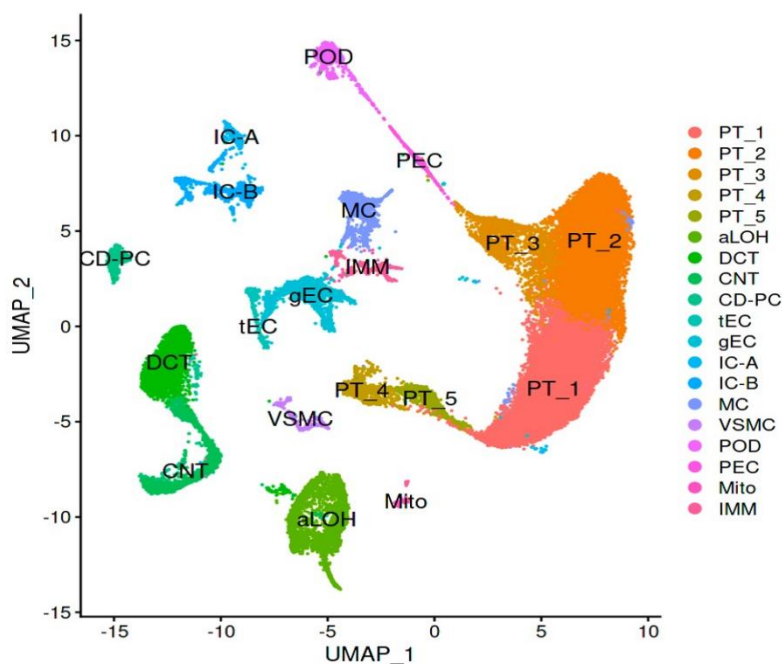
3.2.4 Dot plot of defined marker genes for each cell types

The marker genes that defined each cell type and the unbiased marker genes about each cluster were shown in the dot plot (Figure 16).
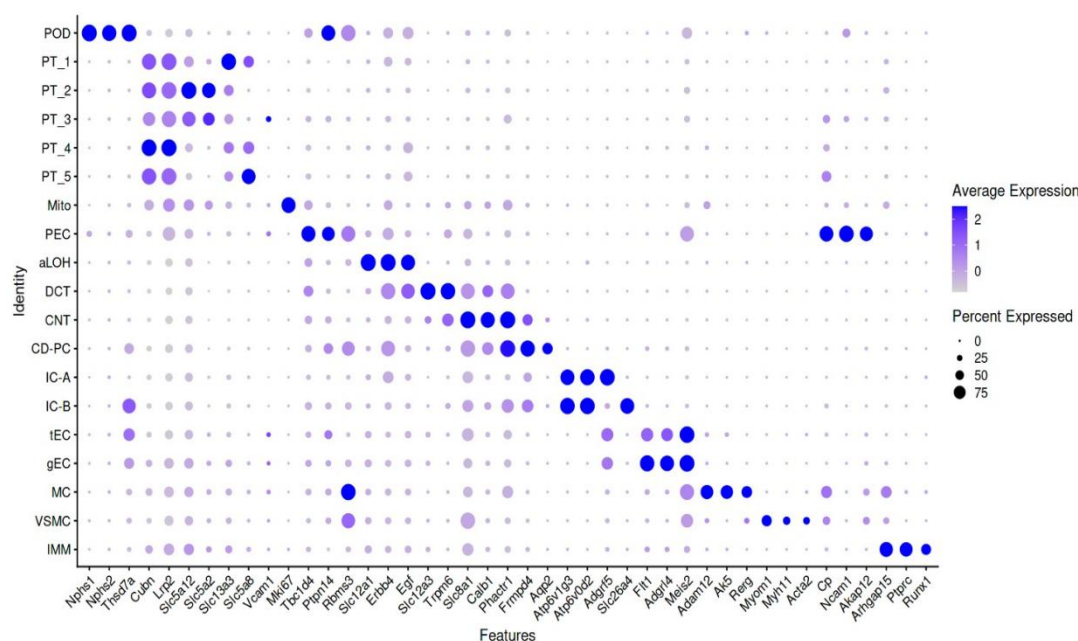
Figure 16. Dot plot of defined marker genes for each cell type. The size of the dots indicated the percentage of each cluster's relative gene expression.

3.2.5 The number of DEGs in different kidney cell types

Next, we analyzed different expression for each cell type by comparing wild-type with the vehicle, and the treatments with the vehicle. A summary of the number of differentially expressed genes (DEGs) in each cell type (Figure 17). By comparing the number of DEGs (nDEGs), we can identify which cell types respond to the treatment more. Our analysis revealed that different treatments had dominant effects on different cell types, and the combined treatment had a

stronger effect than the SGTL2i treatment alone. Additionally, there were more up-regulated DEGs in response to the treatments. These findings suggested that the treatments have varying impacts on different cell types, and the combined treatment may be more effective than the single treatment in regulating gene expression.

A

nDEG Up		WT vs VEH	COMBINE vs VEH	ARB vs VEH	SGLT2i vs VEH
Glom cell types	POD	64	293	127	15
	gEC	84	155	175	9
	MC	50	84	73	16
	PEC	19	46	23	3
PT cell types	PT-1	184	128	125	49
	PT-2	135	155	178	90
	PT-3	139	126	140	44
	PT-4	180	149	78	23
	PT-5	81	129	135	48
DT cell types	aLOH	109	150	205	20
	DCT	64	103	162	16
	CNT	70	178	131	19
	CD-PC	114	246	123	13
	IC-A	122	131	65	3
	IC-B	173	212	121	7
Others	tEC	23	35	28	1
	VSMA	20	16	38	0
	IMM	27	63	12	0
	MITO	0	0	0	0

B

nDEG Down		WT vs VEH	COMBINE vs VEH	ARB vs VEH	SGLT2i vs VEH
Glom cell types	POD	91	82	88	65
	gEC	40	19	103	29
	MC	42	20	67	33
	PEC	1	5	4	0
PT cell types	PT-1	185	156	168	108
	PT-2	116	153	185	96
	PT-3	97	75	88	65
	PT-4	164	73	28	49
	PT-5	24	131	109	79
DT cell types	aLOH	102	90	256	39
	DCT	47	93	185	49
	CNT	41	46	102	25
	CD-PC	56	22	33	28
	IC-A	10	17	15	5
	IC-B	53	54	55	19
Others	tEC	8	4	8	7
	VSMA	3	8	11	1
	IMM	5	5	4	6
	MITO	0	0	0	0

Figure 17. Differential gene expression analysis shows different kidney cell types responding to DN injury and different treatments. The figure shows the number of DEGs that were upregulated (A) and downregulated (B) in the WT and treatment groups compared with the vehicle group.

4. Discussion

The main objective of this project is to explore the renoprotective mechanism associated with SGLT2i in DN and whether there is additional renoprotection when ARB and SGLT2i are combined. We used BTBR ob/ob as a type 2 diabetic mouse model to investigate the molecular mechanisms and cellular changes in DN at the single nuclei level. We evaluated the changes in each kidney nucleus in response to DN when treated with SGLT2i and ARB alone or in combination. Our study indicated that SGLT2i and ARB might protect against different kidney cell types through different signaling pathways. Firstly, we have compared two DEGs between WT versus vehicle and SGLT2i and/or ARB treatments versus vehicle, respectively. We compare the overlapping genes between the two DEGs, which we call responsive genes. We are most interested in responsive genes because they show that SGLT2i and/or ARB treatments succeed in reversing disease-associated genes and the extent alleviated DN.

4.1 Effect of SGLT2i on glomeruli

The glomerular hyperfiltration in early DN is critical for the progressive development of glomerulosclerosis[94]. Maintaining GFR is essential for renal protection. It has been suggested that the reduction of intraglomerular pressure by SGLT2i may produce a renoprotective effect, the underlying molecular mechanism has not been completely elucidated.

Our study showed significant changes in responsive gene expression in glomerular cells, many gene expression directions were reversed after treatment with SGLT2i, ARB, or both. Some responsive genes were regulated

by combination therapy only, suggesting a possible synergistic effect. We investigated the effect of each treatment (alone or combination) on responsive genes in podocyte, MC, and gEC at 12 weeks.

The results showed that the number of significantly upregulated responsive genes in the podocyte, MC, and gEC after SGLT2i treatments were 9, 6, and 6, respectively. The number of responsive genes significantly up-regulated after ARB treatment were 17, 8, 34 respectively. The number of responsive genes significantly up-regulated after combined treatment were 25, 6, 22, respectively. We hypothesized that the responsive gene expression alterations in the podocyte, MC, and gEC segments at 12 weeks may represent the most direct transcriptional effects of different treatments and may provide insight into the molecular mechanisms underlying their protective effects.

In podocytes, the first and most upregulated responsive gene in the SGLT2i treatment group was *Egf*. Epidermal Growth Factor (EGF) family growth factors regulate different epithelial ion channels in the kidney. For instance, EGF stimulates Ca2+ channels via intracellular signaling from PKC and tyrosine kinases and can also regulate sodium transport mediated by renal epithelial Na+ channels (ENaC) [95, 96]. It was found that activation of EGF reduced ENaC activity, protected glomeruli, and tubules by reducing renal perfusion pressure, and delayed the development of hypertension[97]. These results suggest that in podocytes, one of the mechanisms of SGLT2i may be to regulate ion channels to improve renal perfusion to exert a nephroprotective effect[98]. In addition, ARB upregulated *Egf* expression, but combination therapy did not affect *Egf* expression in podocytes.

In gEC, the first and most upregulated responsive gene in the SGLT2i treatment

group was *Bnc2*, which encodes a zinc finger protein that enables alternative splicing of exons and has the potential to generate different mRNA isoforms[99]. Congenital renal and urinary tract anomalies (CAKUT) are a major cause of pediatric ESRD and CKD before the age of 30 years[100]. Variations in the gene *Bnc2* have been identified to cause a type of CAKUT and were associated with diabetic renal complications [100, 101]. These findings suggest that one of the mechanisms of SGLT2i may be to regulate alternative splicing to protect the kidney. In addition, ARB, and combination treatments also upregulated *Bnc2* expression in gEC, suggesting a possible synergistic effect.

In MC, the first and most upregulated responsive gene in the SGLT2i treatment group was *Pde4b*, which is a member of the cyclic nucleotide phosphodiesterase (PDE) family. *Pde4b* is involved in cAMP metabolism and is important for various aspects of cellular physiology, including inflammatory responses, immune responses, and hypertension[102]. *Pde4b* is essential for the precise regulation of cAMP levels to maintain them in an optimal concentration range[103, 104]. A 2 to 4-fold increase in cAMP above basal levels typically produces the greatest physiological response[105]. Consequently, SGLT2i may be to regulate cyclic nucleotide metabolism to protect the kidney. We confirmed that only SGLT2i, but not ARB or combined treatment, rescued *Pde4b* expression in MC.

4.2 Effects of SGLT2i on PT

The direct target cells of SGLT2i are PT cells, and it was found that RAAS plays an essential role in PT cells[106]. Furthermore, many studies indicate that PT cells play a crucial role in the pathogenesis of DN[107, 108].

Our study reveals responsive gene expression in PT cells, many responsive gene expression directions were reversed after treatment with SGLT2i, ARB, or both. Some responsive genes were regulated by combination therapy, suggesting a possible synergistic effect.

We investigated how each treatment, either alone or in combination, altered gene expressions in S1/S2 and S3 segments of PT. The number of responsive genes in the S1/S2 and S3 segments that were significantly up-regulated after SGLT2i treatment were 192 and 181, respectively. The number of responsive genes significantly up-regulated after ARB treatment were 163 and 150 respectively. The number of responsive genes significantly up-regulated after combined treatment were 176 and 236 respectively.

We hypothesized that the responsive gene expression alterations in the S1/S2 and S3 segments at 12 weeks may represent the most direct transcriptional effects of different treatments and may provide insight into the molecular mechanisms underlying their protective effects.

In the S1/S2 segment, the first and most upregulated responsive gene in the SGLT2i treatment group was *Trabd2b*, which encodes a metalloproteinase, a member of the WNT antagonist family that cleaves the WNT amino terminus. It has been demonstrated that sustained activation of WNT-β-catenin signaling leads to renal podocyte damage, aggravated kidney fibrosis, and chronic kidney disease-associated mineral bone disease[109]. These results indicate that one of SGLT2i's mechanisms of action may include modulating the protein coding for protective signaling pathway switches. Meanwhile, ARBs and combined treatment also upregulated *Trabd2b* expression in S1/2 segment.

In the S3 segment, the first and most responsive upregulated gene in the SGLT2i treatment group was *Ifitm7*, which encodes an interferon-induced transmembrane protein (IFITM), a member of the transmembrane protein family[110]. The IFITM family has various functions, including prevention of cellular carcinogenesis, control of cell proliferation, prevention of viral infections *etc.* [111, 112]. However, no studies have reported *Ifitm7* functions. We confirmed that only SGLT2i, but not ARB or combined treatment, rescued *Ifitm7* expression in the S3 segment.

4.3 Effect of SGLT2i on DT and CD

We investigated the extent to which different treatment regimens rescued DN-induced gene expression changes in DT cell types.

In aLOH and DCT, the first most upregulated responsive gene in the SGLT2i-treated group was *Tox*, a nuclear DNA-binding factor that belongs to the high-mobility group box superfamily. *Tox* has been reported to regulate T-cell growth, NK-cell development [113], roles in DNA repair and genome instability[114], cell cycle regulation, etc [115]. These results suggest that the mechanism of SGLT2i may influence various immune cell development processes by regulating DNA binding. We confirmed that ARB and combined treatment also upregulated *Tox* expression in aLOH, and that only SGLT2i, but not ARB or combined treatment rescued *Tox* expression in DCT.

In CNT, the first most upregulated responsive gene in the SGLT2i-treated group was *Arntl*. Transcription factors *Arntl* and Clock drive central oscillators in the hypothalamus and peripheral tissues[116, 117]. Recent research suggests that *Arntl* may contribute to the preservation of normal renal function[118]. In Renal

52

ischemia-reperfusion injury (IRI), *Arntl* protects renal function by regulating mitochondrial homeostasis through modulation of the SIRT1/PGC-1α axis[119]. In addition, it has been shown that *Arntl* deficiency leads to decreased aldosterone levels and blood pressure[120]. These results suggest that one of the mechanisms of SGLT2i may regulate mitochondrial homeostasis to protect renal function. We confirmed that SGLT2i and combined treatment, not ARB rescued *Arntl* expression in CNT.

In CD-PC, IC-A, and IC-B, the first most responsive upregulated gene in the SGLT2i-treated group was *Camk2b*, which is a member of the calcium (2+)/calmodulin-dependent protein kinase subfamily and the serine/threonine protein kinase family. It has been found that *Camk2b* may reduce cell death and fibrosis by upregulating *Chl1* expression[121]. These results suggest that one of the mechanisms of SGLT2i may be involved in regulating cell death and fibrosis to protect renal function. In addition, ARB, and combination treatment also upregulated *Camk2b* expression, suggesting a possible synergistic effect.

In conclusion, based on the characterization of SGLT2i and/or ARB-treated DN mice and primary data of snRNA-seq, it is possible to explore the mechanisms of DN disease progression and gain a deeper understanding of how current therapies slow down disease progression.

4.4 Future perspective

In our study, we intended to investigate the mechanisms of how SGLT2i and RAAS drugs alone or being combined to protect kidney cells. Our research is aimed to explore the underlying mechanisms at the single cell level.

In next steps, we will increase the number of samples for snRNA-seq to achieve the statistical significance and reproduce the results from the primary data. Further analyses of the relevant pathways and upstream regulations based on the treatment specific and common DEGs will be conducted in the future.

5. Summary

In diabetes, glomerular hyper-filtration appears to be driven by SGLT2. Hyper-reabsorption of glucose and sodium in the proximal tubule remarkably reduces sodium delivery to the distal tubule, which is incorrectly sensed by the JGA and consequently leads to limited tubuloglomerular feedback, resulting in increased intraglomerular pressure and glomerular hyper-filtration.

Increasing evidence has reported renal protection after kidney disease-targeted interventions, such as RAAS modulators and SGLT2i, indicating the importance of reducing intraglomerular pressure, which is essential for the preservation of kidney function. This study aims to underlie the mechanism behind the renal protective benefits of SGLT2i and RAAS modulators.

The major findings of this study are summed up as following:

1. 12-weeks SGLT2i and/or ARB treatments showed tendencies to attenuate the albuminuria progression in DN mice.

2. Primary snRNA-seq data were generated with 5 female DN kidneys (n=1 per condition).

3. Differential expression analysis suggested that the SGLT2i and/or ARB treatments had significant effects on different cell types in the kidney.

4. Combined treatment showed stronger effects on kidney cells compared to SGLT2i treatment.

6. Zusammenfassung

Bei Diabetes scheint die glomeruläre Hyperfiltration durch das SGLT2 angetrieben zu werden. Die Hyperresorption von Glukose und Natrium im proximalen Tubulus reduziert die Natriumabgabe an den distalen Tubulus erheblich, was von der JGA falsch wahrgenommen wird und folglich zu einer eingeschränkten tubuloglomerulären Rückkopplung führt, was einen erhöhten intraglomerulären Druck und eine glomeruläre Hyperfiltration zur Folge hat.

Es gibt zunehmend Hinweise auf einen Nierenschutz nach gezielten Eingriffen bei Nierenerkrankungen, wie RAAS-Modulatoren und SGLT2-Inhibitoren, was auf die Bedeutung der Senkung des intraglomerulären Drucks hinweist, der für den Erhalt der Nierenfunktion von wesentlicher Bedeutung ist. Ziel dieser Studie ist es, den Mechanismus hinter den nierenschützenden Vorteilen von SGLT2i und RAAS-Modulatoren zu verstehen.

Die wichtigsten Ergebnisse dieser Untersuchung lassen sich wie folgt zusammenfassen:

1.12-wöchige SGLT2i und/oder ARB-Behandlungen zeigten Tendenzen, das Fortschreiten der Albuminurie bei DN-Mäusen zu vermindern.

2. Primäre Einzelkern-RNA-Sequenzierungsdaten wurden mit 5 weiblichen DN-Nieren erzeugt (n=1 pro Bedingung).

3. Die Analyse der differentiellen Expression deutete darauf hin, dass die SGLT2i- und/oder ARB-Behandlungen signifikante Auswirkungen auf verschiedene Zelltypen in der Niere hatten.

4. kombinierte Behandlung zeigte im Vergleich zur SGLT2i-Behandlung deutlich stärkere Auswirkungen auf die Nierenzellen.

7. Reference

1. Roden, M. and G.I. Shulman, *The integrative biology of type 2 diabetes.* Nature, 2019. **576**(7785): p. 51-60.
2. Khan, M.A.B., et al., *Epidemiology of Type 2 Diabetes - Global Burden of Disease and Forecasted Trends.* J Epidemiol Glob Health, 2020. **10**(1): p. 107-111.
3. Xue, R., et al., *Mechanistic Insight and Management of Diabetic Nephropathy: Recent Progress and Future Perspective.* J Diabetes Res, 2017. **2017**: p. 1839809.
4. Tavafi, M., *Diabetic nephropathy and antioxidants.* J Nephropathol, 2013. **2**(1): p. 20-7.
5. Donate-Correa, J., et al., *Inflammatory Targets in Diabetic Nephropathy.* J Clin Med, 2020. **9**(2).
6. Wolf, G., *New insights into the pathophysiology of diabetic nephropathy: from haemodynamics to molecular pathology.* Eur J Clin Invest, 2004. **34**(12): p. 785-96.
7. Forbes, J.M., et al., *Role of advanced glycation end products in diabetic nephropathy.* J Am Soc Nephrol, 2003. **14**(8 Suppl 3): p. S254-8.
8. Mauer, S.M., M.W. Steffes, and D.M. Brown, *The kidney in diabetes.* Am J Med, 1981. **70**(3): p. 603-12.
9. Mauer, S.M., et al., *Structural-functional relationships in diabetic nephropathy.* J Clin Invest, 1984. **74**(4): p. 1143-55.
10. Kefalides, N.A., *Basement membrane research in diabetes mellitus.* Coll Relat Res, 1981. **1**(3): p. 295-9.
11. Menne, J., et al., *Diminished loss of proteoglycans and lack of albuminuria in protein kinase C-alpha-deficient diabetic mice.* Diabetes, 2004. **53**(8): p. 2101-9.
12. Vernier, R.L., et al., *Heparan sulfate proteoglycan in the glomerular basement membrane in type 1 diabetes mellitus.* Kidney Int, 1992. **41**(4): p. 1070-80.
13. Satchell, S., *The role of the glomerular endothelium in albumin handling.* Nat Rev Nephrol, 2013. **9**(12): p. 717-25.
14. Osterby, R., et al., *Advanced diabetic glomerulopathy. Quantitative structural characterization of nonoccluded glomeruli.* Diabetes, 1987. **36**(5): p. 612-9.
15. Satirapoj, B., *Review on pathophysiology and treatment of diabetic kidney disease.* J Med Assoc Thai, 2010. **93 Suppl 6**: p. S228-41.
16. Kopel, J., C. Pena-Hernandez, and K. Nugent, *Evolving spectrum of diabetic nephropathy.* World J Diabetes, 2019. **10**(5): p. 269-279.
17. Afkarian, M., et al., *Clinical Manifestations of Kidney Disease Among US Adults With Diabetes, 1988-2014.* JAMA, 2016. **316**(6): p. 602-10.
18. Kume, S., et al., *Secular changes in clinical manifestations of kidney disease among Japanese adults with type 2 diabetes from 1996 to 2014.* J Diabetes Investig, 2019. **10**(4): p. 1032-1040.
19. de Boer, I.H. and M.W. Steffes, *Glomerular filtration rate and albuminuria: twin manifestations of nephropathy in diabetes.* J Am Soc Nephrol, 2007. **18**(4): p. 1036-7.
20. Pugliese, G., et al., *Diabetic kidney disease: new clinical and therapeutic issues. Joint*

position statement of the Italian Diabetes Society and the Italian Society of Nephrology on "The natural history of diabetic kidney disease and treatment of hyperglycemia in patients with type 2 diabetes and impaired renal function". J Nephrol, 2020. **33**(1): p. 9-35.

21.   Brosius, F.C. and C.W. Heilig, *Glucose transporters in diabetic nephropathy.* Pediatr Nephrol, 2005. **20**(4): p. 447-51.

22.   Heilig, C.W., et al., *Overexpression of glucose transporters in rat mesangial cells cultured in a normal glucose milieu mimics the diabetic phenotype.* J Clin Invest, 1995. **96**(4): p. 1802-14.

23.   Jakus, V. and N. Rietbrock, *Advanced glycation end-products and the progress of diabetic vascular complications.* Physiol Res, 2004. **53**(2): p. 131-42.

24.   Noh, H. and G.L. King, *The role of protein kinase C activation in diabetic nephropathy.* Kidney Int Suppl, 2007(106): p. S49-53.

25.   Lee, H.B., et al., *Reactive oxygen species-regulated signaling pathways in diabetic nephropathy.* J Am Soc Nephrol, 2003. **14**(8 Suppl 3): p. S241-5.

26.   Koya, D., et al., *Characterization of protein kinase C beta isoform activation on the gene expression of transforming growth factor-beta, extracellular matrix components, and prostanoids in the glomeruli of diabetic rats.* J Clin Invest, 1997. **100**(1): p. 115-26.

27.   Ohshiro, Y., et al., *Reduction of diabetes-induced oxidative stress, fibrotic cytokine expression, and renal dysfunction in protein kinase Cbeta-null mice.* Diabetes, 2006. **55**(11): p. 3112-20.

28.   Ziyadeh, F.N. and G. Wolf, *Pathogenesis of the podocytopathy and proteinuria in diabetic glomerulopathy.* Curr Diabetes Rev, 2008. **4**(1): p. 39-45.

29.   Gnudi, L., S.M. Thomas, and G. Viberti, *Mechanical forces in diabetic kidney disease: a trigger for impaired glucose metabolism.* J Am Soc Nephrol, 2007. **18**(8): p. 2226-32.

30.   Thomson, S.C., V. Vallon, and R.C. Blantz, *Kidney function in early diabetes: the tubular hypothesis of glomerular filtration.* Am J Physiol Renal Physiol, 2004. **286**(1): p. F8-15.

31.   Vallon, V., R. Blantz, and S. Thomson, *The salt paradox and its possible implications in managing hypertensive diabetic patients.* Curr Hypertens Rep, 2005. **7**(2): p. 141-7.

32.   Peti-Peterdi, J., *Calcium wave of tubuloglomerular feedback.* Am J Physiol Renal Physiol, 2006. **291**(2): p. F473-80.

33.   Thomson, S., et al., *Adenosine formed by 5'-nucleotidase mediates tubuloglomerular feedback.* J Clin Invest, 2000. **106**(2): p. 289-98.

34.   Tobe, S.W., P.A. McFarlane, and D.M. Naimark, *Microalbuminuria in diabetes mellitus.* CMAJ, 2002. **167**(5): p. 499-503.

35.   Gerstein, H.C., et al., *Albuminuria and risk of cardiovascular events, death, and heart failure in diabetic and nondiabetic individuals.* JAMA, 2001. **286**(4): p. 421-6.

36.   Keller, C.K., et al., *Renal findings in patients with short-term type 2 diabetes.* J Am Soc Nephrol, 1996. **7**(12): p. 2627-35.

37. Romero, C., M. Orias, and M.R. Weir, *Novel RAAS agonists and antagonists: clinical applications and controversies.* Nature Reviews Endocrinology, 2015. **11**(4): p. 242-252.

38. Rossing, K., et al., *Dual blockade of the renin-angiotensin system in diabetic nephropathy: a randomized double-blind crossover study.* Diabetes Care, 2002. **25**(1): p. 95-100.

39. Morrissey, J.J. and S. Klahr, *Effect of AT2 receptor blockade on the pathogenesis of renal fibrosis.* Am J Physiol, 1999. **276**(1): p. F39-45.

40. Siragy, H.M., et al., *Sustained hypersensitivity to angiotensin II and its mechanism in mice lacking the subtype-2 (AT2) angiotensin receptor.* Proc Natl Acad Sci U S A, 1999. **96**(11): p. 6506-10.

41. Kreisberg, J.I., et al., *High glucose elevates c-fos and c-jun transcripts and proteins in mesangial cell cultures.* Kidney Int, 1994. **46**(1): p. 105-12.

42. Burton, C. and K.P. Harris, *The role of proteinuria in the progression of chronic renal failure.* Am J Kidney Dis, 1996. **27**(6): p. 765-75.

43. Nangaku, M. and T. Fujita, *Activation of the renin-angiotensin system and chronic hypoxia of the kidney.* Hypertens Res, 2008. **31**(2): p. 175-84.

44. Jin, Q., et al., *Oxidative stress and inflammation in diabetic nephropathy: role of polyphenols.* Front Immunol, 2023. **14**: p. 1185317.

45. Samsu, N., et al., *Rosmarinic acid monotherapy is better than the combination of rosmarinic acid and telmisartan in preventing podocyte detachment and inhibiting the progression of diabetic nephropathy in rats.* Biologics, 2019. **13**: p. 179-190.

46. Nie, J.M. and H.F. Li, *Therapeutic effects of Salvia miltiorrhiza injection combined with telmisartan in patients with diabetic nephropathy by influencing collagen IV and fibronectin: A case-control study.* Exp Ther Med, 2018. **16**(4): p. 3405-3412.

47. Kao, M.P., et al., *Oxidative stress in renal dysfunction: mechanisms, clinical sequelae and therapeutic options.* J Hum Hypertens, 2010. **24**(1): p. 1-8.

48. Wellen, K.E. and G.S. Hotamisligil, *Inflammation, stress, and diabetes.* J Clin Invest, 2005. **115**(5): p. 1111-9.

49. Khazim, K., et al., *The antioxidant silybin prevents high glucose-induced oxidative stress and podocyte injury in vitro and in vivo.* Am J Physiol Renal Physiol, 2013. **305**(5): p. F691-700.

50. Duni, A., et al., *Oxidative Stress in the Pathogenesis and Evolution of Chronic Kidney Disease: Untangling Ariadne's Thread.* Int J Mol Sci, 2019. **20**(15).

51. Tavafi, M., *Complexity of diabetic nephropathy pathogenesis and design of investigations.* J Renal Inj Prev, 2013. **2**(2): p. 59-62.

52. Forbes, J.M., M.T. Coughlan, and M.E. Cooper, *Oxidative stress as a major culprit in kidney disease in diabetes.* Diabetes, 2008. **57**(6): p. 1446-54.

53. Brem, A.S., D.J. Morris, and R. Gong, *Aldosterone-induced fibrosis in the kidney: questions and controversies.* Am J Kidney Dis, 2011. **58**(3): p. 471-9.

54. Robles, N.R., et al., *Treatment of proteinuria with lercanidipine associated with renin-angiotensin axis-blocking drugs.* Ren Fail, 2010. **32**(2): p. 192-7.

55. Parving, H.H., et al., *The effect of irbesartan on the development of diabetic nephropathy in patients with type 2 diabetes.* N Engl J Med, 2001. **345**(12): p. 870-8.

56. Viberti, G., N.M. Wheeldon, and V.S.I. MicroAlbuminuria Reduction With, *Microalbuminuria reduction with valsartan in patients with type 2 diabetes mellitus: a blood pressure-independent effect.* Circulation, 2002. **106**(6): p. 672-8.

57. Diabetes, C., et al., *The effect of intensive treatment of diabetes on the development and progression of long-term complications in insulin-dependent diabetes mellitus.* N Engl J Med, 1993. **329**(14): p. 977-86.

58. Gorriz, J.L., et al., *Nephroprotection by Hypoglycemic Agents: Do We Have Supporting Data?* J Clin Med, 2015. **4**(10): p. 1866-89.

59. Chao, E.C. and R.R. Henry, *SGLT2 inhibition--a novel strategy for diabetes treatment.* Nat Rev Drug Discov, 2010. **9**(7): p. 551-9.

60. Wu, H., et al., *Mapping the single-cell transcriptomic response of murine diabetic kidney disease to therapies.* Cell Metab, 2022. **34**(7): p. 1064-1078 e6.

61. Ghezzi, C., D.D.F. Loo, and E.M. Wright, *Physiology of renal glucose handling via SGLT1, SGLT2 and GLUT2.* Diabetologia, 2018. **61**(10): p. 2087-2097.

62. Cai, T., et al., *Sodium-glucose cotransporter 2 inhibition suppresses HIF-1alpha-mediated metabolic switch from lipid oxidation to glycolysis in kidney tubule cells of diabetic mice.* Cell Death Dis, 2020. **11**(5): p. 390.

63. Roder, P.V., et al., *The role of SGLT1 and GLUT2 in intestinal glucose transport and sensing.* PLoS One, 2014. **9**(2): p. e89977.

64. Vallianou, N.G., et al., *Sotagliflozin, a dual SGLT1 and SGLT2 inhibitor: In the heart of the problem.* Metabol Open, 2021. **10**: p. 100089.

65. Takebayashi, K., et al., *Effect of canagliflozin on circulating active GLP-1 levels in patients with type 2 diabetes: a randomized trial.* Endocr J, 2017. **64**(9): p. 923-931.

66. Wang, X.X., et al., *SGLT2 Protein Expression Is Increased in Human Diabetic Nephropathy: SGLT2 PROTEIN INHIBITION DECREASES RENAL LIPID ACCUMULATION, INFLAMMATION, AND THE DEVELOPMENT OF NEPHROPATHY IN DIABETIC MICE.* J Biol Chem, 2017. **292**(13): p. 5335-5348.

67. Fattah, H. and V. Vallon, *The Potential Role of SGLT2 Inhibitors in the Treatment of Type 1 Diabetes Mellitus.* Drugs, 2018. **78**(7): p. 717-726.

68. Vallon, V. and S.C. Thomson, *The tubular hypothesis of nephron filtration and diabetic kidney disease.* Nat Rev Nephrol, 2020. **16**(6): p. 317-336.

69. Vallon, V., et al., *SGLT2 inhibitor empagliflozin reduces renal growth and albuminuria in proportion to hyperglycemia and prevents glomerular hyperfiltration in diabetic Akita mice.* Am J Physiol Renal Physiol, 2014. **306**(2): p. F194-204.

70. Song, P., et al., *Knockout of Na(+)-glucose cotransporter SGLT1 mitigates diabetes-induced upregulation of nitric oxide synthase NOS1 in the macula densa and glomerular hyperfiltration.* Am J Physiol Renal Physiol, 2019. **317**(1): p. F207-F217.

71. Vallon, V. and S. Verma, *Effects of SGLT2 Inhibitors on Kidney and Cardiovascular Function.* Annu Rev Physiol, 2021. **83**: p. 503-528.

72. Wiviott, S.D., et al., *Dapagliflozin and Cardiovascular Outcomes in Type 2 Diabetes.*

N Engl J Med, 2019. **380**(4): p. 347-357.

73. Zinman, B., et al., *Empagliflozin, Cardiovascular Outcomes, and Mortality in Type 2 Diabetes.* N Engl J Med, 2015. **373**(22): p. 2117-28.

74. Wanner, C., et al., *Empagliflozin and Progression of Kidney Disease in Type 2 Diabetes.* N Engl J Med, 2016. **375**(4): p. 323-34.

75. Neal, B., et al., *Canagliflozin and Cardiovascular and Renal Events in Type 2 Diabetes.* N Engl J Med, 2017. **377**(7): p. 644-657.

76. Perkovic, V., et al., *Canagliflozin and Renal Outcomes in Type 2 Diabetes and Nephropathy.* N Engl J Med, 2019. **380**(24): p. 2295-2306.

77. Heerspink, H.J.L., et al., *Dapagliflozin in Patients with Chronic Kidney Disease.* N Engl J Med, 2020. **383**(15): p. 1436-1446.

78. Heerspink, H.J., et al., *Sodium Glucose Cotransporter 2 Inhibitors in the Treatment of Diabetes Mellitus: Cardiovascular and Kidney Effects, Potential Mechanisms, and Clinical Applications.* Circulation, 2016. **134**(10): p. 752-72.

79. Cherney, D.Z., et al., *The effect of empagliflozin on arterial stiffness and heart rate variability in subjects with uncomplicated type 1 diabetes mellitus.* Cardiovasc Diabetol, 2014. **13**: p. 28.

80. Kawanami, D., et al., *SGLT2 Inhibitors as a Therapeutic Option for Diabetic Nephropathy.* Int J Mol Sci, 2017. **18**(5).

81. Terami, N., et al., *Long-term treatment with the sodium glucose cotransporter 2 inhibitor, dapagliflozin, ameliorates glucose homeostasis and diabetic nephropathy in db/db mice.* PLoS One, 2014. **9**(6): p. e100777.

82. Wakisaka, M., *Empagliflozin and Progression of Kidney Disease in Type 2 Diabetes.* N Engl J Med, 2016. **375**(18): p. 1799-1800.

83. Coughlan, M.T., et al., *Mapping time-course mitochondrial adaptations in the kidney in experimental diabetes.* Clin Sci (Lond), 2016. **130**(9): p. 711-20.

84. Sano, M., et al., *Increased Hematocrit During Sodium-Glucose Cotransporter 2 Inhibitor Therapy Indicates Recovery of Tubulointerstitial Function in Diabetic Kidneys.* J Clin Med Res, 2016. **8**(12): p. 844-847.

85. Cherney, D.Z., et al., *Renal hemodynamic effect of sodium-glucose cotransporter 2 inhibition in patients with type 1 diabetes mellitus.* Circulation, 2014. **129**(5): p. 587-97.

86. Perkins, B.A., et al., *Sodium-glucose cotransporter 2 inhibition and glycemic control in type 1 diabetes: results of an 8-week open-label proof-of-concept trial.* Diabetes Care, 2014. **37**(5): p. 1480-3.

87. Cherney, D.Z. and B.A. Perkins, *Sodium-glucose cotransporter 2 inhibition in type 1 diabetes: simultaneous glucose lowering and renal protection?* Can J Diabetes, 2014. **38**(5): p. 356-63.

88. Ruggenenti, P., et al., *Glomerular hyperfiltration and renal disease progression in type 2 diabetes.* Diabetes Care, 2012. **35**(10): p. 2061-8.

89. MacIsaac, R.J., et al., *Nonalbuminuric renal insufficiency in type 2 diabetes.* Diabetes Care, 2004. **27**(1): p. 195-200.

90.   Young, M.D. and S. Behjati, *SoupX removes ambient RNA contamination from droplet-based single-cell RNA sequencing data.* Gigascience, 2020. **9**(12).

91.   Wolock, S.L., R. Lopez, and A.M. Klein, *Scrublet: Computational Identification of Cell Doublets in Single-Cell Transcriptomic Data.* Cell Syst, 2019. **8**(4): p. 281-291 e9.

92.   Luecken, M.D. and F.J. Theis, *Current best practices in single-cell RNA-seq analysis: a tutorial.* Mol Syst Biol, 2019. **15**(6): p. e8746.

93.   Butler, A., et al., *Integrating single-cell transcriptomic data across different conditions, technologies, and species.* Nat Biotechnol, 2018. **36**(5): p. 411-420.

94.   Thomas, M.C., et al., *Diabetic kidney disease.* Nat Rev Dis Primers, 2015. **1**: p. 15018.

95.   Ma, R. and S.C. Sansom, *Epidermal growth factor activates store-operated calcium channels in human glomerular mesangial cells.* J Am Soc Nephrol, 2001. **12**(1): p. 47-53.

96.   Bhalla, V. and K.R. Hallows, *Mechanisms of ENaC regulation and clinical implications.* J Am Soc Nephrol, 2008. **19**(10): p. 1845-54.

97.   Pavlov, T.S., et al., *Deficiency of renal cortical EGF increases ENaC activity and contributes to salt-sensitive hypertension.* J Am Soc Nephrol, 2013. **24**(7): p. 1053-62.

98.   Bollee, G., et al., *Epidermal growth factor receptor promotes glomerular injury and renal failure in rapidly progressive crescentic glomerulonephritis.* Nat Med, 2011. **17**(10): p. 1242-50.

99.   Vanhoutteghem, A. and P. Djian, *The human basonuclin 2 gene has the potential to generate nearly 90,000 mRNA isoforms encoding over 2000 different proteins.* Genomics, 2007. **89**(1): p. 44-58.

100.   Jain, S. and F. Chen, *Developmental pathology of congenital kidney and urinary tract anomalies.* Clin Kidney J, 2019. **12**(3): p. 382-399.

101.   Fernandez-Prado, R., et al., *Expanding congenital abnormalities of the kidney and urinary tract (CAKUT) genetics: basonuclin 2 (BNC2) and lower urinary tract obstruction.* Ann Transl Med, 2019. **7**(Suppl 6): p. S226.

102.   Xu, M., et al., *Inhibition of PDE4/PDE4B improves renal function and ameliorates inflammation in cisplatin-induced acute kidney injury.* Am J Physiol Renal Physiol, 2020. **318**(3): p. F576-F588.

103.   Torphy, T.J., et al., *Identification, characterization and functional role of phosphodiesterase isozymes in human airway smooth muscle.* J Pharmacol Exp Ther, 1993. **265**(3): p. 1213-23.

104.   de Boer, J., et al., *Human bronchial cyclic nucleotide phosphodiesterase isoenzymes: biochemical and pharmacological analysis using selective inhibitors.* Br J Pharmacol, 1992. **106**(4): p. 1028-34.

105.   Zhang, K.Y., et al., *A glutamine switch mechanism for nucleotide selectivity by phosphodiesterases.* Mol Cell, 2004. **15**(2): p. 279-86.

106.   Sinha, A.D. and R. Agarwal, *Clinical Pharmacology of Antihypertensive Therapy for the Treatment of Hypertension in CKD.* Clin J Am Soc Nephrol, 2019. **14**(5): p. 757-764.

107.   Gilbert, R.E., *Proximal Tubulopathy: Prime Mover and Key Therapeutic Target in Diabetic Kidney Disease.* Diabetes, 2017. **66**(4): p. 791-800.

108.   Zeni, L., et al., *A more tubulocentric view of diabetic kidney disease.* J Nephrol, 2017. **30**(6): p. 701-717.

109.   Schunk, S.J., et al., *WNT-beta-catenin signalling - a versatile player in kidney injury and repair.* Nat Rev Nephrol, 2021. **17**(3): p. 172-184.

110.   Miller, L.C., et al., *Evolutionary characterization of pig interferon-inducible transmembrane gene family and member expression dynamics in tracheobronchial lymph nodes of pigs infected with swine respiratory disease viruses.* Vet Immunol Immunopathol, 2014. **159**(3-4): p. 180-91.

111.   Smith, R.A., et al., *Expression of the mouse fragilis gene products in immune cells and association with receptor signaling complexes.* Genes Immun, 2006. **7**(2): p. 113-21.

112.   Lange, U.C., et al., *The fragilis interferon-inducible gene family of transmembrane proteins is associated with germ cell specification in mice.* BMC Dev Biol, 2003. **3**: p. 1.

113.   Vong, Q.P., et al., *TOX2 regulates human natural killer cell development by controlling T-BET expression.* Blood, 2014. **124**(26): p. 3905-13.

114.   Lobbardi, R., et al., *TOX Regulates Growth, DNA Repair, and Genomic Instability in T-cell Acute Lymphoblastic Leukemia.* Cancer Discov, 2017. **7**(11): p. 1336-1353.

115.   Lee, J.H., et al., *Identification and characterization of a novel human PP1 phosphatase complex.* J Biol Chem, 2010. **285**(32): p. 24466-76.

116.   Lowrey, P.L. and J.S. Takahashi, *Mammalian circadian biology: elucidating genome-wide levels of temporal organization.* Annu Rev Genomics Hum Genet, 2004. **5**: p. 407-41.

117.   Kornmann, B., et al., *System-driven and oscillator-dependent circadian transcription in mice with a conditionally active liver clock.* PLoS Biol, 2007. **5**(2): p. e34.

118.   Zhang, D. and D.M. Pollock, *Circadian regulation of kidney function: finding a role for Bmal1.* Am J Physiol Renal Physiol, 2018. **314**(5): p. F675-F678.

119.   Ye, P., et al., *BMAL1 regulates mitochondrial homeostasis in renal ischaemia-reperfusion injury by mediating the SIRT1/PGC-1alpha axis.* J Cell Mol Med, 2022. **26**(7): p. 1994-2009.

120.   Tokonami, N., et al., *Local renal circadian clocks control fluid-electrolyte homeostasis and BP.* J Am Soc Nephrol, 2014. **25**(7): p. 1430-9.

121.   Jia, Q., et al., *Anti-Tumor Role of CAMK2B in Remodeling the Stromal Microenvironment and Inhibiting Proliferation in Papillary Renal Cell Carcinoma.* Front Oncol, 2022. **12**: p. 740051.

8. Appendix

ACE	Angiotensin-converting enzyme
ACEi	Angiotensin-converting enzyme inhibitors
AGE	Advanced glycation end products
Ang I	Angiotensin I
Ang II	Angiotensin II
Ang III	Angiotensin III
Ank3	Ankyrin 3
AP-1	Activator protein 1
AP-1	Activator protein-1
ARBs	Angiotensin II receptor blocker
ARN	Angiotensin receptor–neprilysin;
ART	Afferent arteriole
AT1	Type-1 Ang II receptor
AT2	Type-2 Ang II receptor
CAKUT	Congenital renal and urinary tract anomalies
cAMP	Cyclic AMP
CCA	Canonical Correlation Analysis
CKD	Chronic kidney disease
CREDENCE	Clinical evaluation of renal disease
DAPA-CKD	Dapagliflozin and prevention of adverse outcomes in chronic kidney disease
DEG	Differential gene expression
ECM	Extracellular matrix
EGF	Epidermal growth factor
eGFR	Estimated glomerular filtration rate
ENaC	Epithelial Na+ channels

eNOS	Endothelial nitric oxide synthase
ESL	Endothelial surface layer
GBM	Glomerular basement membrane
gEC	Glomerular endothelial cell
GFB	Glomerular filtration barrier
GFR	Glomerular filtration rate
GLUT	Glucose transporter
HVGs	Highly variable genes
IFITM	Interferon-induced transmembrane protein
IRAP	leucyl-cystinyl aminopeptidase;
IRI	Renal ischemia-reperfusion injury
JGA	Juxtaglomerular apparatus
KNN	K-nearest neighbor
LOX	Lipoxygenase
MAPK	Mitogen-activated protein kinase
MAS1	Proto-oncogene Mas
MC	Mesangial cells
MCP-1	Monocyte chemoattractant protein 1
MNN	Mutual nearest neighbours
MSR2	Macrophage scavenger receptor 2
NDCCB	Non dihydropyridine calcium channel blockers
nDEGs	Significant differentially expressed genes
NF-κB	Nuclear factor κB
NLB	Nuclear lysis buffer
NOX	NADPH oxidase
PAI-1	Plasminogen activator inhibitor-1
PCA	Principal component analysis

PDE	Phosphodiesterase
PKC	Protein kinase C
RAGE	Receptors for AGEs
RAS	Renin-angiotensin system
RH	Recombinant human
RNS	Reactive nitrogen species
ROS	Reactive oxygen species
snRNA-seq	Single-nucleus RNA sequencing
Sp1	Specificity protein 1
TGF	Transforming growth factor β
TMB	Tuber basement membrane
UMAP	Uniform approximation and projection
VEGF	Vascular endothelial growth factor

9. Acknowledgment

10. Curriculum vitae

Personal Information

Name: Zhouning, Liao

Date of Birth: 29/08/1992

Gender: Female

Nationality: Chinese

Language: English, Chinese

Email: 420813477@qq.com

Phone: 017675873518

Educational Background

2020- Present	Doctorate Degree in Medicine (Dr. Med.) Universitätsklinikum Hamburg-Eppendorf, Hamburg, Germany
2016 – 2019	Master of Clinical Medicine Central South University, Changsha, China
2011 – 2016	Bachelor of Clinical Medicine University of South China, Hengyang, China

Awards and Honors

09/2021	China Scholarship Council (CSC) scholarships, China
09/2019	National First-Class Scholarship in Changsha, China
09/2016	National Second-Class Scholarship in Hengyang, China

Publications

1. AAV-based gene therapy to treat inflammatory kidney disease.
   Wu G, Liu S, Hagenstein J, Hengel F, Schaper M, Akyüz N, Alawi M, Liao Z, Failla A, Dierlamm J, Körbelin J, Lu S, Huber T. J Clin Invest (In Revision).

2. Single-cell transcriptomics reveals a mechanosensitive injury signaling. pathway in early diabetic nephropathy.
   Liu S, Zhao Y, Lu S, Zhang T, Lindenmeyer MT, Nair V, Gies SE, Wu G, Nelson RG, Czogalla J, Aypek H, Zielinski S, Liao Z, Schaper M, Fermin D, Cohen CD, Delic D, Krebs CF, Grahammer F, Wiech T, Kretzler M, Meyer-Schwesinger C, Bonn S, Huber TB. Genome Med. 10;15(1):2. (2023)

3. Alpha-mangostin attenuates diabetic nephropathy in association with suppression of acid sphingomyelianse and endoplasmic reticulum stress.
   Liu T, Duan W, Nizigiyimana P, Gao L, Liao Z, Xu B, Liu L, Lei M.
   Biochem Biophys Res Commun.5;496(2):394-400. (2018)

11. Eidesstattliche Versicherung

Ich versichere ausdrücklich, dass ich die Arbeit selbständig und ohne fremde Hilfe verfasst, andere als die von mir angegebenen Quellen und Hilfsmittel nicht benutzt und die aus den benutzten Werken wörtlich oder inhaltlich entnommenen Stellen einzeln nach Ausgabe (Auflage und Jahr des Erscheinens), Band und Seite des benutzten Werkes kenntlich gemacht habe. Ferner versichere ich, dass ich die Dissertation bisher nicht einem Fachvertreter an einer anderen Hochschule zur Überprüfung vorgelegt oder mich anderweitig um Zulassung zur Promotion beworben habe. Ich erkläre mich einverstanden, dass meine Dissertation vom Dekanat der Medizinischen Fakultät mit einer gängigen Software zur Erkennung von Plagiaten überprüft warden kann.

Unterschrift: ....